ELSEVIER

Earth-Science Reviews 54 (2001) 349–392

EARTH-SCIENCE REVIEWS

www.elsevier.com/locate/earscirev

Phanerozoic atmospheric CO_2 change: evaluating geochemical and paleobiological approaches

Dana L. Royer [a,*], Robert A. Berner [a,1], David J. Beerling [b,2]

[a] *Kline Geology Laboratory, Yale University, P.O. Box 208109, New Haven, CT 06520-8109, USA*
[b] *Department of Animal and Plant Sciences, University of Sheffield, Sheffield S10 2TN, UK*

Accepted 8 November 2000

Abstract

The theory and use of geochemical modeling of the long-term carbon cycle and four paleo-PCO_2 proxies are reviewed and discussed in order to discern the best applications for each method. Geochemical models provide PCO_2 predictions for the entire Phanerozoic, but most existing models present 5–10 m.y. means, and so often do not resolve short-term excursions. Error estimates based on sensitivity analyses range from $\pm$75–200 ppmV for the Tertiary to as much as $\pm$3000 ppmV during the early Paleozoic.

The $\delta^{13}C$ of pedogenic carbonates provide the best proxy-based PCO_2 estimates for the pre-Tertiary, with error estimates ranging from $\pm$500–1000 ppmV. Pre-Devonian estimates should be treated cautiously. Error estimates for Tertiary reconstructions via this proxy are higher than other proxies and models ($\pm$400–500 ppmV), and should not be solely relied upon. We also show the importance of measuring the $\delta^{13}C$ of coexisting organic matter instead of inferring its value from marine carbonates.

The $\delta^{13}C$ of the organic remains of phytoplankton from sediment cores provide high temporal resolution (up to 10^3–10^4 year), high precision ($\pm$25–100 ppmV for the Tertiary to $\pm$150–200 ppmV for the Cretaceous) PCO_2 estimates that can be near continuous for most of the Tertiary. Its high temporal resolution and availability of continuous sequences is advantageous for studies aiming to discern short-term excursions. This method, however, must correct for changes in growth rate and oxygen level. At elevated PCO_2 ($\sim$ 750–1250 ppmV), this proxy loses its sensitivity and is not useful.

The stomatal density and stomatal index of land plants also provide high temporal resolution ($< 10^2$ year), high precision ($\pm$10–40 ppmV for the Tertiary and possibly Cretaceous) PCO_2 estimates, and so also is ideal for discerning short-term excursions. Unfortunately, this proxy also loses sensitivity at some level of PCO_2 above 350 ppmV (which, currently, is largely undetermined).

Our analysis of the recently developed $\delta^{11}B$ technique shows that it currently is not yet well constrained. Most importantly, it requires the assumption that the boron isotopic composition of the ocean remains nearly constant through

* Corresponding author. Fax: +1-203-432-3134.
E-mail addresses: dana.royer@yale.edu (D.L. Royer), robert.berner@yale.edu (R.A. Berner), D.J.Beerling@Sheffield.ac.uk (D.J. Beerling).
[1] Fax: +1-203-432-3134.
[2] Fax: +44-0114-222-0002.

PII: S0012-8252(00)00042-8

time. In addition, it assumes that there are no biological or temperature effects and that diagenetic alteration of the boron isotopic composition does not occur.

A fifth CO_2 proxy, based on the redox chemistry of marine cerium, has several fundamental flaws and is not discussed in detail here.

Keywords: carbon dioxide; paleoatmosphere; paleoclimatology; indicators

1. Introduction

During the last decade, numerous methods for evaluating past concentration of atmospheric carbon dioxide (PCO_2) have been developed and/or refined. The most reliable method has been the determination of the composition of air trapped in glacial ice (e.g., Friedli et al., 1986; Petit et al., 1999). However, this method is only useful for the past 400 ka because of the absence of ice older than this. Thus, other methods have been applied to the older geologic record. Quantifying paleo-CO_2 is vital for

Nomenclature:

Symbols commonly used in text

C_a^*	PCO_2
C_s^*	soil CO_2 (mol cm^3)
$C_{37:2}$	diunsaturated long-chained alkenones
D_s^*	diffusion coefficient for soil CO_2 (cm^2 s^{-1})
p_i/p_a	ratio of internal:ambient CO_2
S	CO_2 contributed by biological respiration
z	depth in a soil profile (cm)
$\bar{z}$	characteristic CO_2 production depth (cm)
α_{diff} and ε_{diff}	fractionation factor for diffusion during carbon fixation (‰)
α_f and ε_f	kinetic fractionation factor for carbon fixation (‰)
α_P and ε_P	combined fractionation for carbon fixation (‰)
δ_a	$\delta^{13}C$ of the atmosphere (‰)
δ_{cc}	$\delta^{13}C$ of pedogenic carbonate (‰)
δ_i	$\delta^{13}C$ of CO_2 at the site of carbon fixation (‰)
δ_{occ}	$\delta^{13}C$ of marine carbonate (‰)
δ_{om}	$\delta^{13}C$ of organic matter (‰)
δ_p	$\delta^{13}C$ of photosynthate (‰)
δ_s	$\delta^{13}C$ of soil CO_2 (‰)
δ_ϕ	$\delta^{13}C$ of soil-respired CO_2 (‰)
$\delta_{\Sigma B}$	$\delta^{11}B$ of total dissolved B (‰)
ε	free air porosity in soil
ε_a	ambient atmospheric partial pressure of water vapor
ε_i	intercellular partial pressure of water vapor
ϕ_s^*	CO_2 production rate (mol s^{-1} cm^{-3})
μ	growth rate (d^{-1})
ρ	tortuosity

understanding climate dynamics, most notably its effect on global temperature (e.g., Sloan and Rea, 1995; Kothavala et al., 1999) through the so-called 'greenhouse effect'. PCO_2 affects many other aspects of the biosphere including particularly the physiology, productivity and distribution of terrestrial vegetation. This in turn influences our interpretation of the plant fossil record (Beerling, 1998b) and exerts an important impact on the feedback between vegetation and climate by changing the exchange of energy and water vapor between the land surface and the overlying atmosphere (e.g., Bounoua et al., 1999). Quantifying the PCO_2 of the ancient atmosphere, therefore, provides a firmer basis for assessing the linkages between PCO_2 and the biosphere that are urgently required for understanding the geologic past (Beerling, 2000).

Here, we critically consider the underlying theory, practice, and applicability of geochemical modeling of the long-term (multimillion year) carbon cycle and four paleo-PCO_2 proxies. Several of the proxies were developed for and first applied to the Quaternary, but their application to the pre-Quaternary record will be emphasized here. The four proxies are the $\delta^{13}C$ of phytoplankton, the $\delta^{13}C$ of pedogenic carbonates (including the goethite method), stomatal density and stomatal index, and the $\delta^{11}B$ of marine calcium carbonate. In considering the applicability of the various approaches to the geologic record, their associated temporal resolutions and precision of PCO_2 estimates will be emphasized.

2. Geochemical modeling of the long-term carbon cycle

The level of atmospheric CO_2 over geologic time can be estimated by constructing mass balance expressions for all the processes that bring about inputs and outputs of CO_2 to and from the atmosphere. This is a daunting task at any timescale. The best one can do is to construct theoretical models and attempt to devise rates and rate laws for processes involved in the carbon cycle and how these rates may have changed over time. Since this review is concerned with pre-Quaternary PCO_2, only models that treat CO_2 changes over millions of years will be discussed. The carbon cycle on a multimillion year basis is dominated by the exchange of carbon between rocks and the surficial reservoir consisting of the atmosphere + biosphere + oceans + soils, and the processes involved in the long-term cycle are different from those that are involved in the short-term cycle, which considers only the exchange of carbon within the surficial reservoir (see Berner, 1999).

Because the amount of CO_2 in the atmosphere is exceedingly small compared to the carbon fluxes into and out of it, it is very difficult to calculate changes in PCO_2 due to imbalances between these fluxes over millions of years (Berner and Caldeira, 1997). Calculations of PCO_2 from imbalances via time-dependent modeling have been made (Berner et al., 1983; Lasaga et al., 1985), but they require treatment of fluxes of additional elements such as Ca, Mg, and S, as well as fluxes of carbon between the ocean and atmosphere as well as between rocks and the surficial reservoir. Because of their complexity, these models will not be covered here. Instead, simpler models dealing only with carbon, principally the GEOCARB and similar models (Budyko et al., 1987; Berner, 1991, 1994; Caldeira and Kasting, 1992; François and Walker, 1992; Kump and Arthur, 1997; Tajika, 1998; Berner and Kothavala, 2001; Wallman, 2001), will be discussed. Several other modeling approaches to the long-term carbon cycle have been made, but they do not actually calculate CO_2 concentrations and will not be discussed here (Walker et al., 1981; Caldeira, 1992; Raymo and Ruddiman, 1992; Godderis and François, 1995, 1996; Derry and France-Lanord, 1996; France-Lanord and Derry, 1997; Gibbs et al., 1997, 1999; Kump and Arthur, 1999; McCauley and DePaolo, 1997; Raymo, 1997; François and Godderis, 1998).

The GEOCARB model considers the input of CO_2 to the atmosphere from the thermal breakdown of carbon in rocks resulting in volcanic, metamorphic, and diagenetic degassing. Additional CO_2 input comes from the weathering of organic matter in rocks exposed on the continents. Carbon dioxide is removed from the atmosphere by the weathering of Ca–Mg silicate and carbonate minerals to form dissolved bicarbonate in groundwater, followed by transport of the HCO_3^- by rivers to the oceans where the HCO_3^- is removed as Ca–Mg carbonates in bottom sediments. Thus, carbon is transferred from the atmosphere to carbonate rocks. In some models

(e.g., Wallman, 2001), direct weathering of Ca–Mg silicates to carbonates on the seafloor is also considered. The burial of organic matter in both marine and non-marine sediments also removes CO_2 fixed by photosynthesis from the atmosphere.

Because the mass of carbon exchanging with rocks via volcanism, weathering, etc., over millions of years is so much larger than that present at any given time in the surficial reservoir (atmosphere + biosphere + oceans + soils), it can be assumed that for each large time step in the calculation the sum of fluxes from rocks to the surficial system are essentially equal to the sum of fluxes back to the rocks. This is what is done in GEOCARB modeling and it is this assumption of quasi-steady state that allows the calculation of PCO_2 over geologic time. It represents the reasonable idea that extremely large masses of carbon, that would otherwise result if the fluxes did not balance, cannot be stored in any portion of the surficial reservoir (for example, the continents can accommodate just so much biomass, and excess HCO_3^- in the oceans will eventually precipitate as $CaCO_3$ due to excessive supersaturation—see Berner and Caldeira, 1997 for further discussion).

2.1. Method of calculation

Carbon cycle models treat a large variety of processes and, therefore, involve mathematical treatment that is far more complex than that used for the other paleo-CO_2 proxies discussed elsewhere in the present review. For this reason, the entire GEOCARB model is not presented here but only summarized qualitatively with a minimum of mathematical expressions. Further details of the modeling can be found in the original papers (Berner, 1991, 1994; Berner and Kothavala, 2001; variants of GEOCARB-type modeling are presented by others referenced above, but they rest on similar reasoning). The fundamental basis of the GEOCARB model is two carbon mass balance equations:

$$F_{wc} + F_{mc} + F_{wg} + F_{mg} = F_{bc} + F_{bg} \quad (1)$$

$$\delta_c(F_{wc} + F_{mc}) + \delta_g(F_{wg} + F_{mg}) = \delta_{bc}F_{bc} + (\delta_{bc} - \alpha_c)F_{bg} \quad (2)$$

where: F_{wc}, F_{wg} = rate of release of carbon to the atmosphere + biosphere + oceans + soils system via the weathering of carbonates (c) and organic matter (g); F_{mc}, F_{mg} = rate of release of carbon to the atmosphere + biosphere + oceans + soils; system via the metamorphic/volcanic/diagenetic breakdown of carbonates (c) and organic matter (g); F_{bc}, F_{bg} = burial rate of carbon as carbonates (c) and organic matter (g) in sediments; δ_c, $\delta_g = \delta^{13}C$ value (per mil) for carbonates (c) and organic matter (g) undergoing weathering; $\delta_{bc} = \delta^{13}C$ value (per mil) for carbonates undergoing burial in sediments; α_c = carbon isotope fractionation (per mil) between organic matter and carbonates both undergoing burial in sediments. These equations represent the quasi-steady state equivalence of the sum of CO_2 inputs and outputs for each time step in the modeling (for GEOCARB the time step is 1 million year).

From these equations and additional algebraic expressions for each of the input fluxes (terms on the left-hand side of the equations), and how they change with time, one can solve the two equations for each flux F as a function of time. This requires data on the following subjects as they affect continental weathering: total land area and mean continental elevation (from paleogeographic maps), relative areas of exposure of silicate vs. carbonate rocks (from paleogeologic reconstructions), global river runoff (from general circulation climate models (GCMs) applied to ancient paleogeographies), land temperature (from GCMs), the rise of large vascular land plants and their quantitative effect on weathering (from modern weathering studies), the effect of solar evolution on mean global temperature and river runoff (from GCMs), the effect of changes in PCO_2 on climate and river runoff (atmospheric greenhouse effect from GCMs), and the effect of changes in PCO_2 on the rate of growth and weathering by land plants (from modern plant experiments).

Inputs of CO_2 to the atmosphere are parameterized in the GEOCARB model in terms of: seafloor spreading rate as a guide to global tectonic degassing (from seafloor area/age relations and paleo-sea level data), and the rise of calcareous plankton as they affect the amounts of $CaCO_3$ in deep sea sediments subjected to heating and degassing during plate subduction. Organic carbon and calcium carbonate burial rates in sediments are derived from the carbon iso-

topic record of carbonates being buried at each time step and Eqs. (1) and (2) above. A summary of these factors considered by the GEOCARB model is shown in Table 1.

The calculation of PCO_2 in GEOCARB modeling (sensu strictu) is derived by determining the rate of weathering of Ca–Mg silicates on land to Ca–Mg carbonates in the oceans. This is equivalent to $F_{bc} - F_{wc}$ from Eq. (1). The expression for silicate weathering is:

$$F_{wsi}(t) = F_{bc} - F_{wc} = f_B(t)\, f_H(t)\, f_R(t)\, f_E(t)\, f_D(t)^{0.65} F_{wsi}(0) \quad (3)$$

where: $F_{wsi}(t)$ = rate of Ca–Mg silicate weathering with ultimate conversion to Ca–Mg carbonates; the value for the present is designated as $F_{wsi}(0)$; $f_H(t)$ = effect on weathering of global mean land temperature at some past time (t)/present global mean land temperature; $f_R(t)$ = effect on weathering rate of mean continental relief at time (t)/mean continental relief at present; $f_E(t)$ = dimensionless parameter expressing the dependence of weathering rate on soil biological activity due to land plants ($f_E(t) = 1$ at present); $f_D(t)$ = river runoff (t)/river runoff at present due to changes in paleogeography; $f_B(t)$ = dimensionless feedback factor representing the effects of CO_2 and temperature on weathering rate.

The value of $F_{wsi}(0)$ can be estimated from modern river water data and values of $f_R(t)$, $f_H(t)$, $f_E(t)$, and $f_D(t)^0$ are obtained via the methods outlined above. With these results Eq. (3) can then be solved for $f_B(t)$. The parameter $f_B(t)$ represents the effects on silicate mineral weathering of changes in temperature and runoff as they are, in turn, affected by changes in PCO_2 and solar radiation. Also included is the effect of PCO_2 on plant-mediated weathering. The parameter $f_B(t)$ represents negative feedback against a runaway greenhouse or icehouse climate. Derivation of the resulting complex algebraic expression for $f_B(t)$ allows solution of it for PCO_2 once the actual value of $f_B(t)$ has been determined.

Table 1
Outline of processes in the GEOCARB II model (after Berner, 1991, 1994)

Weathering of silicates, carbonates, and organic matter
(1) Topographic relief as affected by mountain uplift (silicates and organic matter)
(2) Global land area (carbonates)
(3) Global river runoff and land temperature as affected by changes in continental area and position
(4) Relative areas of land underlain by silicates vs. carbonates
(5) Rise and evolution of vascular land plants
(6) Enhancement of weathering flux by changes in global temperature and runoff
  (a) Due to evolution of the sun
  (b) Due to changes in atmospheric CO_2 (greenhouse effect)
(7) Enhancement of plant-mediated weathering due to fertilization by atmospheric CO_2

Thermal degassing of CO_2 from volcanism, diagenesis, and metamorphism
(1) Changes in global seafloor spreading rate
(2) Transfer of $CaCO_3$ between platforms and the deep sea

Burial of organic matter and carbonates in sediments
(1) Calculated via mass balance from sum of input fluxes
(2) Relative proportions derived from carbon isotopic data

2.2. Problems with the method

A large number of assumptions go into GEOCARB and the similar models of Caldeira and Kasting (1992) and Tajika (1998). Simple error analysis is impossible but a rough idea of error can be determined by sensitivity analysis. This was done in the GEOCARB modeling (Berner, 1991, 1994; Berner and Kothavala, 2001) by varying each of the values for $f_R(t)$, $f_E(t)$, etc., from no change from the present to geologically extreme maximum and minimum values and examining the effect on CO_2. For example, varying the effect of different groups of land plants on chemical weathering of Ca–Mg silicates results in large changes in calculated CO_2 level (Berner, 1991, 1994; Berner and Kothavala, 2001). Varying groups of related parameters, such as the assumption of no change in tectonic degassing, no change in paleogeography, no evolution of land plants, etc., has also been done. Such sensitivity analysis has allowed the construction of crude error margins for the "best estimate" of CO_2 concentration over Phanerozoic time. The error margins are large and show that the "best estimates" are probably good to only a factor of about two (see Fig. 13).

Another problem lies with the limits of temporal resolution. Data are input into the GEOCARB model

every 10 million years (every 5 million years for some Cenozoic isotopic data). As a result, the model cannot delineate short-lived events such as the Permo-Triassic and Cretaceous-Tertiary (K–T) extinction, the late Ordovician glaciation, and the Paleocene–Eocene (P–E) $\delta^{13}C$ excursion. The GEOCARB model is intended to treat only more gradual changes over many millions of years. However, this does not preclude the application of similar carbon cycle mass balance modeling to shorter timescales as has been done by Gibbs et al. (1997) for the late Ordovician glaciation.

Even with sensitivity analysis the model calculations are no better than the various assumptions made by the GEOCARB model. Some of the larger problems, ranked in order of more-to-less serious, are:

1. The content of $CaCO_3$ in subducting sediments is virtually unknown before the Jurassic (150 Ma).
2. The estimate of paleorelief, and its effect on weathering, is poorly known.
3. Seafloor spreading rates before the Jurassic are not represented simply by changes in sea level, as is assumed by the model.
4. River runoff and land temperature calculations are based on GCM calculations for flat continents. Recalculation based on realistic topography is needed.
5. The effect of large shifts in the proportions of basalt vs. granite weathering has not been evaluated.
6. Little is known of how changes from gymnosperms to angiosperms affected the rate of plant-mediated weathering.
7. Global degassing may not scale linearly with seafloor spreading rate as assumed.
8. Other factors have been ignored (midplate superplume degassing, seafloor basalt weathering, etc.).

2.3. Summary

The carbon cycle modeling method has many inherent problems, but it at least considers and discusses the processes that actually bring about changes in atmospheric CO_2 over geologic time. It is always amenable to modification and improvement. The method is best evaluated by its agreement or lack of agreement with the other methods. As an example, there is surprisingly good agreement, within error ranges for each method, between the PCO_2 values calculated via GEOCARB modeling and those derived from the study of carbonate paleosols (see Fig. 14).

3. $\delta^{13}C$ of phytoplankton

The carbon isotopic composition of biomass is a function of the carbon source, the carbon assimilation pathway, and the biosynthesis and metabolism of the assimilated organic carbon. In sedimentary organic matter, diagenetic processes may also be important. In the case of autotrophs, the carbon assimilation pathway often strongly alters the carbon isotopic signature relative to the carbon source. For example, the equilibrium and kinetic isotope effects associated with photosynthesis consistently fractionate strongly against ^{13}C. One factor that affects these fractionations in phytoplankton is the concentration of CO_2 dissolved in water ($[CO_{2(aq)}]$) (Degens et al., 1968; McCabe, 1985). This relationship is often inverted and applied to the geologic past to estimate paleoatmospheric CO_2, ranging from the late Triassic to Quaternary (Popp et al., 1989; Jasper and Hayes, 1990; Freeman and Hayes, 1992; Pagani et al., 1999a,b).

3.1. Photosynthetic fractionation of ^{13}C

Two processes fractionate the carbon pool during photosynthesis: the equilibrium isotope effect of CO_2 diffusion at the boundary layer of the photosynthesizer, and the kinetic isotope effect of CO_2 fixation. The difference in diffusivity for two isotopes in a given gas is proportional to the square root of their reduced masses (Mason and Marrero, 1970); in air, $^{13}CO_2$ is 4.4‰ less diffusive than $^{12}CO_2$ (Craig, 1953), and for water the difference is 0.7‰ (O'Leary, 1984). This fractionation factor can be expressed as the following:

$$\alpha_{\text{diff}} = \frac{1000 + \delta_a}{1000 + \delta_i} \quad (4)$$

where α_{diff} = fractionation due to diffusion, $\delta_a = \delta^{13}C$ of the atmosphere, and $\delta_i = \delta^{13}C$ at the site of fixation. The kinetic effect associated with carbon fixation is usually driven by rubisco (ribulose-1,5-biphosphate carboxylase oxygenase), the enzyme that catalyzes the reaction between RuBP (ribulose-1,5-biphosphate) and CO_2 to form PGA (3-phosphoglyceric acid), a 3-carbon acid. In vitro, there is a 29‰ fractionation against ^{13}C at 25°C (Roeske and O'Leary, 1985). In vivo, however, the value for vascular plants is closer to 27‰ (Evans et al., 1986; Farquhar et al., 1982) and 25‰ for phytoplankton (Laws et al., 1995; Bidigare et al., 1997; Popp et al., 1998; Hayes et al., 1999). These discrepancies are likely due to both a drop in CO_2 from the intercellular spaces to the site of fixation and a $\approx 10\%$ of total carbon fixation via PEP carboxylase, an enzyme that only mildly fractionates against ^{13}C (Farquhar and Richards, 1984). The kinetic fractionation factor can be expressed as the following:

$$\alpha_f = \frac{1000 + \delta_i}{1000 + \delta_p} \quad (5)$$

where α_f = kinetic fractionation associated with carbon fixation, and $\delta_p = \delta^{13}C$ of the photosynthate.

Although the fractionations associated with photosynthesis are highly invariant, for a given δ_a, δ_p can vary by as much as 15‰, particularly for photosynthesizers in stressed environments (e.g., water stress in land plants, nutrient stress). Farquhar et al. (1982) proposed that this variation is principally a function of the ratio of internal CO_2 to ambient CO_2 (p_i/p_a). In essence, the $\delta^{13}C$ of inorganic carbon within photosynthesizers follows a Rayleigh distillation process, with p_i/p_a controlling how closed the system is. This relationship can be expressed as the following (after Farquhar et al., 1982; Popp et al., 1989):

$$\alpha_p = \alpha_{diff} + (\alpha_f - \alpha_{diff})\, p_i/p_a \quad (6)$$

where α_p = fractionation factor integrating the two isotopic fractionations described above (Eqs. (4) and (5)). This can be recast in terms of ε values, where $\varepsilon \equiv (\alpha - 1) \times 10^3$:

$$\varepsilon_p \equiv \varepsilon_{diff} + (\varepsilon_f - \varepsilon_{diff})\, p_i/p_a. \quad (7)$$

For phytoplankton, the following values for ε_{diff} and ε_f can be substituted (see above):

$$\varepsilon_p \equiv 0.7 + 24.3\, p_i/p_a. \quad (8)$$

In most vascular plants, stomata (pores through which plants exchange gases and other constituents with the atmosphere) help regulate CO_2 within their mesophyll. If the CO_2 external to a leaf rises or carbon assimilation rates drop, stomata-bearing plants respond by reducing their stomatal pore area, and vice-versa, so that p_i/p_a usually remains at approximately 0.7 (Polley et al., 1993; Ehleringer and Cerling, 1995; Beerling, 1996; Bettarini et al., 1997; Arens et al., 2000), particularly for unstressed plants. Phytoplanktons lack stomata and consequently have less control over p_i/p_a. Furthermore, the diffusion of CO_2 in water is about 10^4 times slower than in air, suggesting again less internal control over p_i/p_a. One might, therefore, expect a stronger correlation in phytoplankton between $[CO_{2(aq)}]$ and ε_p.

3.2. Correlation between $[CO_{2(aq)}]$ and ε_P

McCabe (1985) experimentally quantified the relationship between $[CO_{2(aq)}]$ and ε_p using mixed algal populations from several New Zealand lakes:

$$\varepsilon_p = (17.0 \pm 2.2)\log\left[CO_{2(aq)}\right] - 3.4$$
$$2 \le \left[CO_{2(aq)}\right] \le 74\,\mu M \quad (9)$$

where the uncertainty represents the 95‰ confidence interval. Rau et al. (1989, 1991b) measured δ_p and calculated $[CO_{2(aq)}]$ for the South Atlantic/Weddell Sea and the Drake Passage, and found the following relationships:

$$(\text{S. Atlantic})\ \delta_a = -0.8\left[CO_{2(aq)}\right] - 12.6$$
$$8 < \left[CO_{2(aq)}\right] < 24\,\mu M \quad (10)$$

$$(\text{Drake Passage})\ \delta_a = -0.90\left[CO_{2(aq)}\right] - 9.40$$
$$15 < \left[CO_{2(aq)}\right] < 23\,\mu M. \quad (11)$$

Jasper and Hayes (1990) established a similar relationship using reconstructed ε_p values from a late Quaternary hemipelagic sediment core and cor-

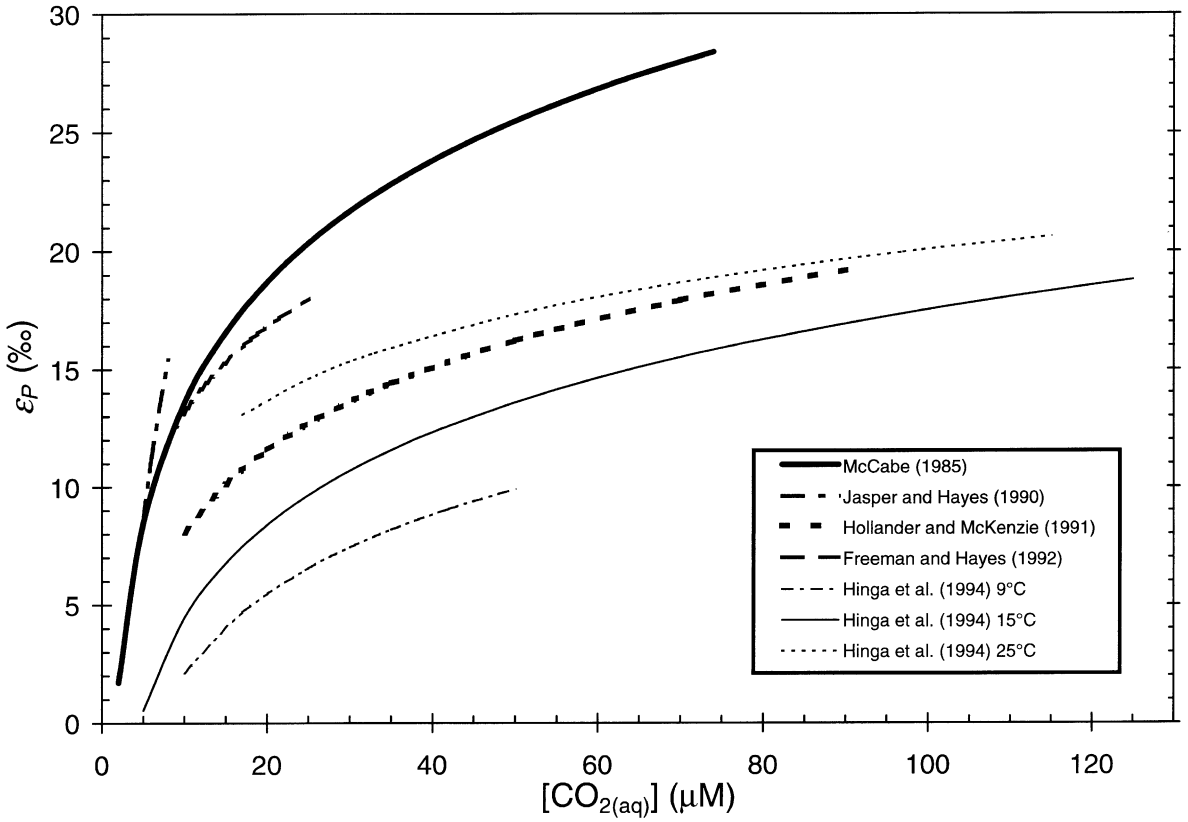

Fig. 1. Reported values for the relationship between ε_p and $[CO_{2(aq)}]$ using various techniques and settings (oceanic and lacustrine). Equations given in text (Eqs. (9), (12)–(17)).

responding $[CO_{2(aq)}]$ values calculated from the Vostok ice core:

$$\varepsilon_p = 32.9\log\left[CO_{2(aq)}\right] - 14.3$$
$$5 < \left[CO_{2(aq)}\right] < 8\,\mu M. \quad (12)$$

Hollander and McKenzie (1991) also generated an estimate of this relationship, calculating $[CO_{2(aq)}]$ and ε_p over an annual cycle in Lake Greifen, Switzerland:

$$\varepsilon_p = 11.64\log\left[CO_{2(aq)}\right] - 3.56$$
$$10 < \left[CO_{2(aq)}\right] < 90\,\mu M. \quad (13)$$

Freeman and Hayes (1992) compiled GEOSECS data from several ocean basins, and found the following relationship between calculated $[CO_{2(aq)}]$ and ε_p:

$$\varepsilon_p = 12.03\log\left[CO_{2(aq)}\right] + 1.19$$
$$8 < \left[CO_{2(aq)}\right] < 25\,\mu M. \quad (14)$$

Hinga et al. (1994) experimentally grew the diatom *Skeletonema costatum* at three temperatures. After accounting for possible pH effects, the following relationships were observed:

$$(9°C)\ \varepsilon_p = 11.21\log\left[CO_{2(aq)}\right] + 8.99$$
$$10 < \left[CO_{2(aq)}\right] < 50\,\mu M \quad (15)$$
$$(15°C)\ \varepsilon_p = 13.06\log\left[CO_{2(aq)}\right] + 8.58$$
$$5 < \left[CO_{2(aq)}\right] < 125\,\mu M \quad (16)$$
$$(25°C)\ \varepsilon_p = 9.09\log\left[CO_{2(aq)}\right] + 1.89$$
$$17 < \left[CO_{2(aq)}\right] < 115\,\mu M. \quad (17)$$

The results of the five studies solving for ε_p are shown in Fig. 1. Significant variations among the estimates exist. Using Henry's law to convert $[CO_{2(aq)}]$ to PCO_2 (after Freeman and Hayes, 1992; see Section 3.5), Miocene ε_p values of 15.8‰

(Freeman and Hayes, 1992) yield a PCO_2 estimate of 400 ppmV using the regression of McCabe (1985) but 1400 ppmV using Hollander and McKenzie (1991); early Cretaceous values of 21.2‰ (Freeman and Hayes, 1992) yield an estimate of 1000 ppmV using McCabe (1985) but 4900 ppmV using Hollander and McKenzie (1991). Beyond the differences among these logarithmic relationships, it is not clear based on the above discussion whether the relationship between $[CO_{2(aq)}]$ and ε_P should be logarithmic or linear (Rau et al., 1991a; Freeman and Hayes, 1992). This will be discussed in detail below (Section 3.4).

3.3. Determining paleo-ε_P

As defined above (Eq. (7)), ε_P represents the fractionation of ^{13}C due to photosynthesis. For most modern phytoplankton, ε_P ranges between 10‰ and 20‰. Calculating this value is not straightforward, particularly in fossil material where p_i/p_a is unknown. Instead, modern relationships between what can be measured (e.g., carbonates, organic carbon) and ε_P are used to infer paleo-ε_P. Fig. 2 shows the modern isotopic relationships between ε_P and carbonates and organic carbon.

The use of bulk organic carbon to estimate ε_P (Arthur et al., 1985; Dean et al., 1986; Kump et al., 1999) likely leads to erroneous estimates of paleo-CO_2 (Hayes et al., 1989b; Pagani et al., 2000) due both to the input of terrigenous organic matter and non-primary marine photosynthate. As discussed above (Section 3.1), terrestrial plants are better equipped to regulate p_i/p_a, and as a consequence their carbon isotopic variability over geologic time (where large PCO_2 fluctuations likely occurred) is much smaller than that for marine organic carbon (Dean et al., 1986; but see Bocherens et al., 1993; Jones, 1994). Likewise, carbon isotopic trends in non-photosynthetic organic material will also not likely follow the phytoplankton trend because their carbon is, at best, several steps removed from primary marine photosynthate.

In response to this limitation, specific biomarkers for photosynthesis have been identified and measured in lieu of bulk organic matter (Hayes et al., 1987, 1989b; Jasper and Hayes, 1990). Geoporphyrins, derived from the aromatic nucleus of chlorophyll (Ekstrom et al., 1983; Hayes, 1993), are one such biomarker used in paleoatmospheric CO_2 reconstructions (Popp et al., 1989; Freeman and Hayes, 1992). While terrestrial plants are a potential source of geoporphyrins, the presence of geoporphyrins in marine settings is probably negligible (Hayes et al., 1989b). The appropriate isotopic pathways are shown in Fig. 2. In modern plants, geoporphyrin precursors (e.g., chlorophyllide) are enriched in ^{13}C relative to bulk biomass by ≈ 0.5‰ (Hayes et al., 1987). Based on theoretical considerations, the conversion of this precursor to geoporphyrins probably does not involve any isotopic fractionation. If a fractionation does exist (e.g., preferential decomposition of ^{12}C) it may, for example, be expected to be large in highly oxygenated environments (Hayes et al., 1989b). The effects of thermal diagenesis have also been shown to be negligible, and can always be verified by comparing geoporphyrin $\delta^{13}C$ values with those of another class of compounds, for example geolipids (Hayes et al., 1989a).

Diunsaturated long-chained alkenones ($C_{37:2}$) are also used as a biomarker (Jasper and Hayes, 1990; Jasper et al., 1994; Pagani et al., 1999a,b), but are preserved in sediments back only to the Cenomanian (ca. 95 Ma) (Farrimond et al., 1986), and are scarce in pre-Neogene sediments. Unlike geoporphyrins, $C_{37:2}$ alkenones are specific to certain haptophytic algae (Prymnesiophyceae) (Conte et al., 1994), ensuring that their isotopic signatures are not diluted by terrestrial contaminants. Thus, when using these alkenones, one can eliminate the $[CO_{2(aq)}]$–ε_P rela-

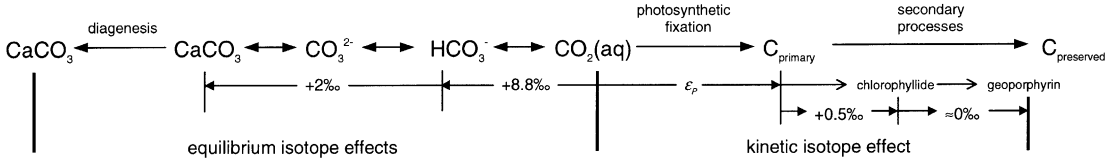

Fig. 2. Isotopic relationships between preserved carbonates and organic matter. Values are for $\delta^{13}C$. Modified after Hayes et al. (1989b).

tionships not based solely on these haptophytic algae (see Fig. 1). In the modern open-ocean, $C_{37:2}$ alkenones are only synthesized by *Emiliania huxleyi* and its relative *Gephyrocapsa oceanica* (Marlowe et al., 1990; Conte et al., 1994), both of which are most common at mid-latitudes. Laboratory analyses find $C_{37:2}$ alkenones $\approx 4‰$ lighter than bulk haptophytic biomass (Jasper and Hayes, 1990; Bidigare et al., 1997; Popp et al., 1998). In addition, the unsaturation ratios of C_{37} alkenones ($[C_{37:2}]/[C_{37:2} + C_{37:3}]$) are correlated with temperature (Brassell et al., 1986; Prahl and Wakeham, 1987), and have been useful for alkenone-based paleo-CO_2 work in the Quaternary (Jasper et al., 1994), but not the Miocene (Pagani et al., 1999a).

As shown in Fig. 2, at least two fractionations exist between $CO_{2(aq)}$ and preserved carbonates. $CO_{2(aq)}$ is enriched in $\delta^{13}C$ when converted to HCO_3^- and again further to calcite. A common value assigned to these combined fractionations (at 25°C) is 10.8‰ (e.g., Popp et al., 1989; see Fig. 2). This value can vary among species, for example, 9.3‰ for *Globigerinoides ruber* at 24°C (Jasper and Hayes, 1990). The fractionations are also temperature dependent, and recent paleo-CO_2 studies have used shallow water $\delta^{18}O$ reconstructed temperatures to solve for these fractionation factors (Freeman and Hayes, 1992; Pagani et al., 1999a,b). One quantification of this dependency is (after Romanek et al., 1992; Mook et al., 1974, respectively):

$$\varepsilon_{\text{calcite}} - CO_{2(g)} = 11.98 - 0.12T(°C) \quad (18)$$

$$\varepsilon_{CO_{2(aq)}} - CO_{2(g)} = 0.19 - 373/T(K) \quad (19)$$

so that at 25°C, $\varepsilon = 10.0‰$.

Diagenetic processes such as reprecipitation and differential dissolution can also affect isotopic compositions. The presence of recognizable nannofossils and frequency of bioturbation and incomplete cementation are typically used to gauge the severity of diagenesis (Hayes et al., 1989b; Pagani et al., 1999a). Comparison of Sr/Ca ratios with that in unaltered contemporaneous calcite can also be used (Hayes et al., 1989b) since Sr/Ca ratios are lower in non-biogenic calcite than in biogenic calcite (Baker et al., 1982).

Given the above guidelines, ε_p can be calculated as follows:

$$\varepsilon_p \equiv \left[\frac{\delta_d + 1000}{\delta_p + 1000} - 1\right] \times 1000 \approx \delta_d - \delta_p \quad (20)$$

where $\delta_d = \delta^{13}C$ of $CO_{2(aq)}$, and $\delta_p = \delta^{13}C$ of the bulk primary photosynthate. Assuming no carbonate diagenesis, δ_d can be calculated from the organic matter's associated calcite. Assuming no secondary processing of the organic biomarker, δ_p can be calculated from the biomarker. For geoporphyrins, the corresponding fractionation factor is $\approx 0.5\%$, and for $C_{37:2}$ alkenones, $\approx 4‰$. Thus, using the alkenone biomarker for sediments with a shallow water paleotemperature of 25°C and the fractionation factors in Eqs. (18) and (19), ε_p can be estimated by:

$$\varepsilon_p = \left[\frac{\delta_d + 990}{\delta_p + 996} - 1\right] \times 1000. \quad (21)$$

3.4. Other confounding factors in determining ε_P

As discussed above (see Eq. (7)), ε_p is a function of p_i/p_a, where p_a represents $[CO_{2(aq)}]$ just outside the boundary layer of the cell. This CO_2 need not equal the global mean concentration, e.g., in areas of upwelling or in stagnant, stratified waters (Popp et al., 1989; Freeman and Hayes, 1992; Goericke et al., 1994). The global mean $[CO_{2(aq)}]$ is required to accurately estimate PCO_2 (see Section 3.5). One approach to minimize this potential bias is sampling sites associated with low productivity (Pagani et al., 1999a,b).

Different species may fractionate carbon differently during photosynthesis. Hinga et al. (1994) found ε_p values 8–10‰ lighter in *E. huxleyi* (a haptophytic alga) than in *S. costatum* (a diatom) under identical conditions. This problem can be largely removed by using $C_{37:2}$ alkenones, since their production is restricted to one taxon.

At low $[CO_{2(aq)}]$, some types of phytoplankton appear to actively transport HCO_3^- (Hinga et al., 1994; Laws et al., 1995, 1997; Popp et al., 1998; but see Bidigare et al., 1997). Laws et al. (1995) concluded that the diatom *Phaeodactylum tricornutum*

probably actively transports HCO_3^- when $[CO_{2(aq)}] < 10$ μM. Bidigare et al. (1997) and Laws et al. (1997) report a similar threshold for other species. If the conversion from bicarbonate to carbon dioxide occurs intracellularly, the subsequent enhanced growth rate (see Fig. 3) will likely offset the heavy carbon supplied by the HCO_3^- (Laws et al., 1995). If the conversion occurs extracellularly, the resulting elevated growth rate is still expected but the $[CO_{2(aq)}]$ supplied by the bicarbonate will probably be similar to the bulk CO_2. This, in turn, may affect ε_p (Laws et al., 1995). This extracellular conversion of HCO_3^- to $CO_{2(aq)}$ is probably the most common active pathway (Laws et al., 1997). Additionally, many types of phytoplankton fix HCO_3^- with PEP carboxylase, which lead to lower ε_p values (see Section 3.1). Most importantly, this rate of fixation may depend on $[CO_{2(aq)}]$, and thus covary with PCO_2 (Hinga et al., 1994; Reinfelder et al., 2000).

Growth rate (Fry and Wainwright, 1991) and cell geometry (Popp et al., 1998) can also influence ε_p. If p_i is purely supplied by diffusion in phytoplankton (i.e., no active transport), the growth rate μ (d^{-1}) is proportional to the difference between p_a and p_i:

$$\mu = k_1 p_a - k_2 p_i. \quad (22)$$

If this is solved for p_i and substituted into Eq. (7), the following relationship is found where growth rate is negatively correlated with ε_p (Rau et al., 1992; François et al., 1993; Goericke et al., 1994; Laws et al., 1995; Bidigare et al., 1997, 1999b; but see Hinga et al., 1994; Popp et al., 1998, 1999):

$$\varepsilon_p = \varepsilon_{diff} + (\varepsilon_f - \varepsilon_{diff})(k_1 - \mu/p_a)/k_2. \quad (23)$$

This equation provides a mechanism for the logarithmic behavior previously observed when ε_p was

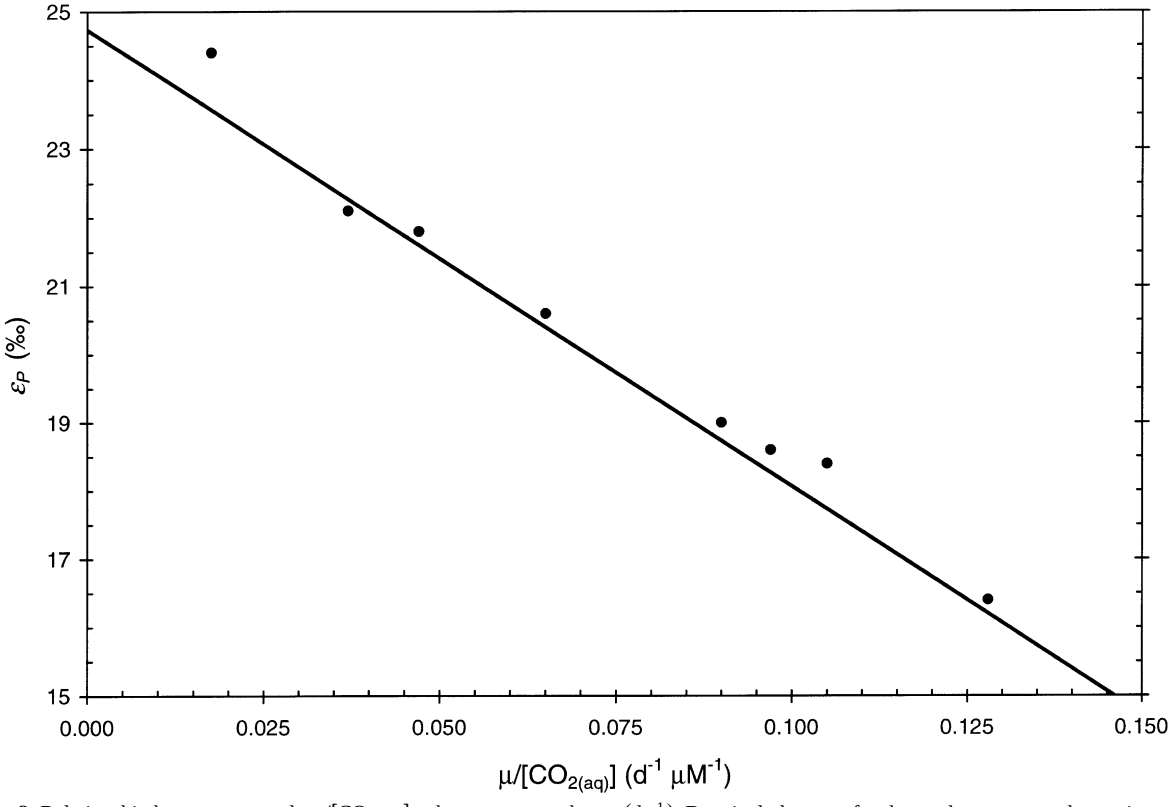

Fig. 3. Relationship between ε_p and $\mu/[CO_{2(aq)}]$, where μ = growth rate (d^{-1}). Data include mean for the modern ocean and experimental results under light:dark cycles of 24:0 and 12:12 h. Regression equation for 24:0-h cycle: $y = -0.015x + 0.371$ ($n = 5$; $r^2 = 0.97$). Data from Laws et al. (1995).

plotted against p_a ($[CO_{2(aq)}]$) (Fig. 1). In contrast, a linear relationship exists between ε_p and $\mu/[CO_{2(aq)}]$ (Fig. 3). Since experimental ε_p values are consistently $\approx 25‰$ when $\mu/[CO_{2(aq)}] = 0$ (Laws et al., 1995; Bidigare et al., 1997; Popp et al., 1998; see Fig. 3), k_1 and k_2 must be proportional to each other. The slopes, however, need not be equal for different species. Popp et al. (1998) calculated, however, that a 20-fold difference in slope among four species when experimentally plotting ε_p vs. $\mu/[CO_{2(aq)}]$ was removed when cell geometry (i.e., cellular carbon content to surface area ratio) was considered. Popp et al. (1999) observed similar behavior in the modern Southern Ocean. Thus, k_1/k_2 may largely be a function of the carbon content to cell surface area ratio.

Fossil studies are generally limited in quantifying growth rate and cell geometry. Bidigare et al. (1997, 1999a) observed a striking correlation ($r^2 = 0.82$) in modern oceans between $[PO_4^{3-}]$ and ε_p, and ascribed the covariation to growth rates. Assuming a ε_p maximum of 25‰, this relationship is as follows:

$$(25 - \varepsilon_p)\left[CO_{2(aq)}\right] = 158\left[PO_4^{3-}\right] + 49. \qquad (24)$$

Pagani et al. (1999a,b) assumed $k_1 = k_2$, solved Eq. (23) for μ, then substituted Eq. (24) for μ in Eq. (23). Fossil sites were then carefully selected to correspond with stable, low productivity areas in the present-day so that modern $[PO_4^{3-}]$ values for these areas could be applied to the fossil sites. Given these $[PO_4^{3-}]$ estimates, ε_p could then be calculated. Bidigare et al. (1997) suggested Cd/Ca ratios might also be useful as a $[PO_4^{3-}]$ proxy. Cell geometry is more difficult to quantify in fossil studies, where in modern plankton can be approximated by their volume to surface area ratio (Popp et al., 1998). This variable may be insignificant in $C_{37:2}$ alkenone studies, however, since they are restricted to a few species that in modern oceans show little volume to surface area variation (Pagani et al., 1999a). Thus, assuming $k_1 = k_2$ in these studies may not introduce large errors. In addition, ε_p in alkenone-producing species appears insensitive to growth rate (Popp et al., 1998).

Hinga et al. (1994) demonstrated that a shift in pH from 7.9 to 8.3 induced a ε_p change of 10‰. Little other evidence concerning this factor exists. Although virtually impossible to observe or calculate, changes in cell membrane diffusivity could also affect ε_p (Goericke et al., 1994). Finally, the diatom *P. tricornutum* was recently found to discriminate more strongly against ^{13}C (1.4‰) in a 32.5% vs. 22% O_2 atmosphere (Berner et al., 2000). The effect is ascribed to carbon recycling via photorespiration, which is partially a function of the O_2 to CO_2 ratio. This ratio was probably higher than today during the late Paleozoic and lower during, for example, the early and mid-Mesozoic (Berner and Canfield, 1989; Berner et al., 2000). Since photorespiration in modern phytoplankton is low (Burns and Beardall, 1987), this effect may only be important for late Paleozoic reconstructions.

3.5. Converting $[CO_{2(aq)}]$ to PCO_2

Once $[CO_{2(aq)}]$ is calculated, it must be converted to PCO_2. According to Henry's law, this relationship is a partial function of temperature. For example, the increase in $[CO_{2(aq)}]$ solubility with decreasing temperature explains the anomalously high $[CO_{2(aq)}]$ and corresponding ε_p values at high latitudes (Rau et al., 1989, 1991b; Popp et al., 1999; Andrusevich et al., 2000). Salinity also influences this relationship, but is generally disregarded in paleostudies (e.g., Pagani et al., 1999a,b). One also assumes equilibrium between $CO_{2(aq)}$ and atmospheric CO_2 (e.g., Freeman and Hayes, 1992; Pagani et al., 1999a,b). Large sections of the modern ocean are up to ± 50 ppmV out of equilibrium with the atmosphere (Tans et al., 1990), and slightly larger values have been calculated for the Quaternary (Jasper et al., 1994), making this a dangerous assumption. Pagani et al. (1999a,b) selected low productivity sites, which typically are closest to equilibrium with respect to CO_2.

3.6. Summary

Several studies have estimated paleoatmospheric CO_2 from the $\delta^{13}C$ of marine phytoplankton, both for the Quaternary (Jasper and Hayes, 1990; Rau et al., 1991a; Jasper et al., 1994) and pre-Quaternary (Freeman and Hayes, 1992; Pagani et al., 1999a,b). Interestingly, White et al. (1994) used an analogous technique for mosses, which lack foliar stomata, spanning the Holocene.

Many relationships and assumptions are required to estimate PCO_2 from the $\delta^{13}C$ of phytoplankton. Pagani et al. (1999a) propagated errors from their estimates of $[PO_4^{3-}]$ (± 0.1 μM), temperature (± 2°C), salinity (35 ± 1‰), ε_f (26 ± 1‰), slope and intercept of $[PO_4^{3-}]$–μ relationship (11%, representing the 95% confidence interval in the modern dataset), and analytical error for $\delta^{13}C_{37:2}$ (± 0.5‰) and $\delta^{13}C_{calcite}$ (± 0.2‰), and calculated an error envelope for PCO_2 of 15%. This error envelope is not likely to decrease substantially in future studies since the ε_p–$[CO_{2(aq)}]$ relationship for $C_{37:2}$ alkenones is currently the most reliable. As discussed above (Section 3.4), its reliability stems from the narrow range of species producing the alkenones, the species' narrow range of cell geometry, and their observed insensitivity (in terms of ε_p) to growth rate. Pagani et al. (1999a,b) also selected stable, low productivity sites, which help minimize non-climatically driven fluctuations of $[CO_{2(aq)}]$ due to processes such as upwelling. Such settings also minimize variation in growth rate and cell geometry (Popp et al., 1998). $[CO_{2(aq)}]$ in regions of low productivity are also more likely to be in equilibrium with PCO_2. Pagani et al. (1999a,b) estimated PCO_2 from a site (ODP 588) with relatively high paleo-surface sea temperatures (15–22°C). Due to the higher concentrations of $CO_{2(aq)}$ in colder water, ε_p in cold water phytoplankton is less sensitive to PCO_2 (François et al., 1993; Popp et al., 1999), and thus warm water sites are preferable.

One drawback to the use of $C_{37:2}$ alkenones is their relative scarcity in many sediments, particularly at higher latitudes and in pre-Neogene sediments (Marlowe et al., 1990). For pre-Cenomanian sites, where $C_{37:2}$ alkenones are unknown, another biomarker is required, which at present would decrease the precision of PCO_2 estimates. A general drawback to the use of marine phytoplankton as a PCO_2 indicator is its decreased precision at high PCO_2, where ε_p asymptotically approaches 25‰. This break in slope usually occurs between 750 and 1250 ppmV CO_2 (Kump and Arthur, 1999).

The temporal resolution of this proxy can be quite high, particularly in densely sampled ocean sediment cores (e.g., Pagani et al., 1999a,b). In the case of Pagani et al. (1999a), the average sampling density was approximately 200 ka. The time that each sample integrated is less in most cases. This temporal resolution exceeds both geochemical models (Section 2) and the method of pedogenic carbonates (Section 4), but is generally less than the method of stomatal parameters (Section 5). The precision of individual PCO_2 estimates is also quite high (± 8–15% in the cases of Freeman and Hayes, 1992; Pagani et al., 1999a,b). Again, this level of precision exceeds that of models and pedogenic carbonates, but is generally exceeded by stomatal parameters.

4. $\delta^{13}C$ of pedogenic carbonates

4.1. The model

In regions receiving less than approximately 800 mm annual precipitation, pedogenic carbonates (i.e., authigenic carbonates in soils) are common (Royer, 1999). In the case of $CaCO_3$, the principal source of calcium is wind-blown dust and dissolved Ca^{2+} in rainwater (Gile et al., 1979). The carbonate ion is typically inherited from biological respired CO_2 (e.g., organic decomposition, root respiration), not carbonate weathering or groundwater CO_2 (Cerling et al., 1989; Quade et al., 1989). This is because the rate of pedogenic carbonate formation is 10^2 to 10^3 times slower than the rate of soil respiration (Cerling, 1984, 1999). Since this biological CO_2 flux dominates (hereafter referred to as soil-respired CO_2), soil CO_2 in well-aerated soils can be modeled as a standard diffusion–production equation (Baver et al., 1972; Kirkham and Powers, 1972; Cerling, 1984):

$$\frac{\partial C_s^*}{\partial t} = D_s^* \frac{\partial^2 C_s^*}{\partial z^2} + \phi_s^*(z) \quad (25)$$

where C_s^* = soil CO_2 (mol cm^{-3}), z = depth in the soil profile (cm), and ϕ_s^* = CO_2 production rate as a function of depth (mol s^{-1} cm^{-3}). D_s^* = diffusion coefficient for CO_2 in the soil (cm^2 s^{-1}), and is calculated as follows:

$$D_s^* = D_{air}\varepsilon\rho \quad (26)$$

where D_{air} = diffusion of CO_2 in the atmosphere, which is a function of pressure and temperature, ε = free air porosity in the soil ($0 < \varepsilon \leq 1$), and ρ = tortuosity factor ($\approx$ permeability, where $0 < \rho \leq 1$). D_s^* is assumed constant with depth (Cerling, 1991).

The CO_2 production term (ϕ_s^*) is modeled to exponentially decay with depth (Dörr and Münnich, 1990), such that:

$$\phi_s^*(z) = \phi_s^*(0)\exp(-z/\bar{z}) \quad (27)$$

where $\bar{z}$ = characteristic CO_2 production depth (cm) (Cerling, 1991). The model is insensitive whether $\phi_s^*(z)$ exponentially decays, linearly decays, or remains constant, so long as the characteristic depth ($\bar{z}$) is correct (Solomon and Cerling, 1987). $\bar{z}$ is not highly constrained in modern soils (Cerling, 1991); however, Dörr and Münnich (1990) report values of 10–20 cm for forested soils; deeper values can be expected in grasslands (Cerling, 1991).

Under steady-state conditions, Eq. (25) equals zero. Given the following boundary conditions: $C_s^*(0) = C_a^*$ where $C_a^* = PCO_2$, and $C_s^*(L) = k$ where L is the depth of an impermeable boundary (e.g., groundwater table) and k is a constant, the general solution to Eq. (25) is (Cerling, 1991):

$$C_s^*(z) = S(z) + C_a^* \quad (28)$$

where $S(z)$ represents the concentration of CO_2 contributed by biological respiration, and is given as:

$$S(z) = \frac{\phi_s^*(0)\,\bar{z}^2}{D_s^*}\left[1 - \exp(-z/\bar{z})\right]. \quad (29)$$

Thus, soil CO_2 represents a mixture of atmospheric and soil-respired CO_2. Eq. (28) can be recast in terms of the $\delta^{13}C$ of C_s^* (Cerling, 1984, 1991). This transformation involves the assumption that soil-respired CO_2 has the same isotopic composition as soil organic matter. The resulting expression is:

$$\delta_s(z) = \left(\frac{1}{R_{PDB}}\left[\frac{S(z)\frac{D_s^*}{D_s^{13}}\left(\frac{R_\phi}{1+R_\phi}\right) + C_a^*\left(\frac{R_a}{1+R_a}\right)}{S(z)\left(1-\frac{D_s^*}{D_s^{13}}\right)\left(\frac{R_\phi}{1+R_\phi}\right) + \left(\frac{C_a^*}{1+R_a}\right)}\right] - 1\right) \times 1000 \quad (30)$$

where $\delta_s = \delta^{13}C$ of soil CO_2, D_s^{13} = diffusion coefficient of $^{13}CO_2$ in soil ($cm^2\ s^{-1}$), and R_ϕ, R_a, and $R_{PDB} = {}^{13}C/{}^{12}C$ ratios of soil-respired CO_2, atmospheric CO_2, and the PDB standard, respectively. Note that the terms enclosed within the inner brackets in Eq. (30) represent the $^{13}C/^{12}C$ ratio of soil CO_2 (δ_s) (Cerling, 1999).

Eqs. (28) and (30) can be transformed and simplified to solve for C_a^*, the concentration of atmospheric CO_2 (Davidson, 1995; Cerling, 1999). The resulting expression is:

$$C_a^* = S(z)\frac{\delta_s - 1.0044\delta_\phi - 4.4}{\delta_a - \delta_s} \quad (31)$$

where δ_ϕ and $\delta_a = \delta^{13}C$ of soil-respired CO_2 and atmospheric CO_2, respectively.

4.2. Patterns in $\delta^{13}C$ of pedogenic carbonate in modern soil profiles

If pedogenic carbonates form in equilibrium with soil CO_2, their $\delta^{13}C$ values (δ_{cc}) can be used as a proxy for δ_s. δ_{cc} measurements in modern soils (formed during the Holocene) validate this assumption (Quade et al., 1989; Cerling et al., 1991a). Fig. 4 shows the striking correlation between field measurements from one soil profile from Nevada (Quade et al., 1989) and the equilibrium-based model prediction (Cerling, 1984). Fig. 4 also verifies the underlying assumption that δ_s (and, by extension, δ_{cc}) is determined by the diffusion of atmospheric and soil-respired CO_2, with little influence from groundwater, parent material, or kinetic or Rayleigh distillation fractionations. If this condition were not met, one would expect heavier δ_{cc} values and more variation at depth. Cerling et al. (1989) measured δ_{cc} and the $\delta^{13}C$ of coexisting organic matter (δ_{om}) in 10 modern soils at depth, where the contribution of δ_a under today's PCO_2 levels is minimal. δ_{cc} was enriched 14–16‰ relative to δ_{om}, consistent with the equilibrium fractionations between these two components.

The sharp decrease in δ_{cc} at shallow soil depths is typical, and represents mixing between heavy δ_a and light δ_ϕ. $\partial\delta_s/\partial z$ approaches zero by 50 cm soil depth in most pedogenic carbonate-producing soils (Cerling, 1984; Ekart et al., 1999). Thus, in paleosol work where z is not known precisely, one must control for this variability by ensuring that measured carbonates are at least 50 cm from the paleosurface. At times of high PCO_2, this asymptotic value of δ_{cc} will shift to heavier values, and vice-versa for times of low PCO_2.

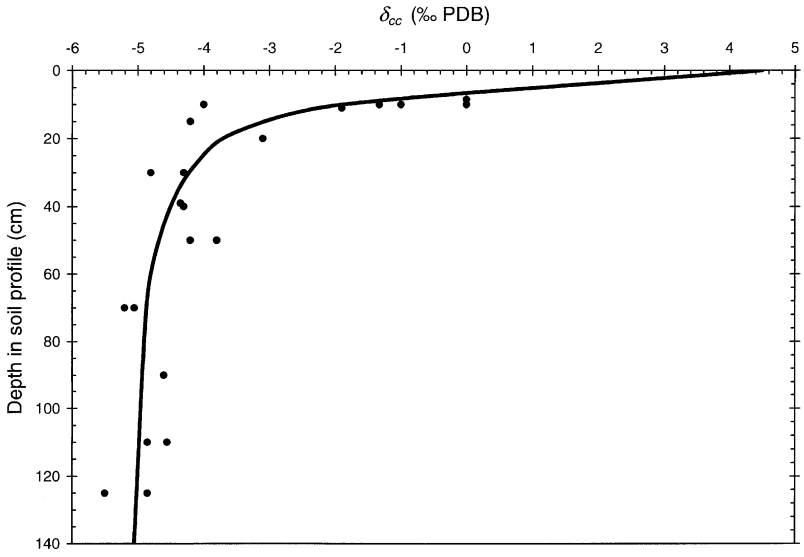

Fig. 4. Measurements of $\delta^{13}C$ of pedogenic carbonate (δ_{cc}) as a function of depth from one soil profile. This soil profile developed on limestone parent material. Solid line represents model prediction based on best estimates of soil temperature, ε, ρ, $\bar{z}$, $\phi_s^*(z)$, δ_ϕ, and δ_a. Figure redrawn from Quade et al. (1989).

4.3. Estimating S(z)

The estimation of atmospheric CO_2 from Eq. (30) hinges on a number of relationships and associated assumptions. The components of $S(z)$ must be estimated, namely soil temperature, pressure, porosity (ε), tortuosity (ρ), characteristic CO_2 production depth ($\bar{z}$), and soil CO_2 respiration rate ($\phi_s^*(0)$). The model is particularly sensitive to ε, $\bar{z}$, and $\phi_s^*(0)$. For example, using a typical modern pedogenic carbonate-forming soil (Cerling, 1991) with a δ_{cc} of -7‰, a $\bar{z}$ of 10 cm yields a PCO_2 estimate of 2500 ppmV, but increases to 5000 ppmV for a $\bar{z}$ of 20 cm. Fortunately, excursions in one or more of these six variables is often balanced by shifts in one or more of the other variables (Cerling, 1999). Therefore, it is not unreasonable to combine these factors and estimate $S(z)$ directly. $S(z)$, as presented above, is the component of C_s^* from soil respiration. This value is not well constrained in modern soils, but current data suggest values of $S(z)$ at depths >50 cm for pedogenic carbonate-producing soils of 3000–5000 and 5000–9000 ppmV for low and high productivity soils, respectively (Brook et al., 1983; Solomon and Cerling, 1987; Cerling, 1999). Again, using a typical modern soil with a δ_{cc} of -7‰, a $S(z)$ of 3000 ppmV yields a PCO_2 estimate of 2000 ppmV, but increases to 5500 ppmV for a $S(z)$ of 9000 ppmV (see Fig. 5).

Carbonates can form at depth in waterlogged gleyed soils. Such soils can have values of $S(z)$ exceeding 25,000 ppmV, causing overestimation of PCO_2 (Cerling, 1991). Thus, soils with gleyed features should be avoided. Pedogenic carbonates also form in desert soils, which typically have values of $S(z)$ below 3000 ppmV (Cerling, 1991) and should also be avoided. Desert soils usually have neither pedogenic carbonates at depths exceeding 50 cm (Royer, 1999) nor well-developed leached horizons. Conversely, non-desert soils rarely have pedogenic carbonates within the upper 20 cm of the profile (Cerling, 1991).

No pattern in the current literature emerges between the $S(z)$ chosen for model calculations and the environmental context of the paleosol. Values for $S(z)$ range from 3000 to 5000 (Ghosh et al., 1995; Lee, 1999), 3000 to 7000 (Mora et al., 1996), 5000 to 10,000 (Mora et al., 1991; Cerling, 1992b; Lee and Hisada, 1999), and 10,000 ppmV (Andrews et al., 1995). As discussed above, pertinent values of $S(z)$ for pedogenic carbonate-forming soils are not well constrained, but highly productive soils have values closer to 9000 ppmV while less productive soils lie closer to 3000 ppmV. Given the sensitivity

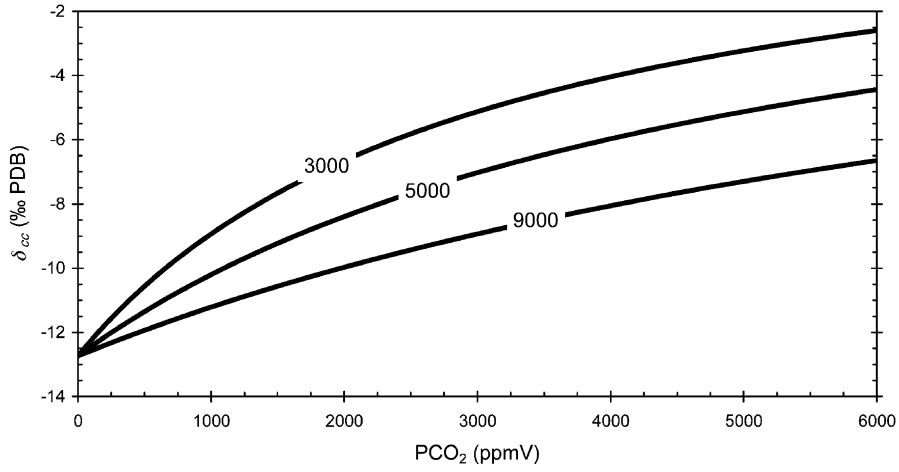

Fig. 5. Sensitivity of PCO_2 estimates to $S(z)$. The three plotted values of $S(z)$ span the expected range for pedogenic carbonate-forming soils. Note that sensitivity increases with heavy pedogenic carbonate $\delta^{13}C$ values (δ_{cc}) (i.e., high PCO_2). Lines drawn from Eq. (31) assuming $\Delta_{cc-s} = 9.0‰$, $\delta_a = -6.5‰$, and $\delta_\phi = -26\%$.

of the model to this variable, more research is required.

Recently, Ekart et al. (1999) compiled published and unpublished δ_{cc} data and calculated PCO_2 for 68 paleosol sites. Many variables were standardized to facilitate more direct comparison among the sites. A value for $S(z)$ of 5000 ppmV was uniformly applied, which given our poor understanding of $S(z)$ is not unreasonable, but surely significant variation in $S(z)$ existed among the 68 sites.

4.4. Estimating δ_ϕ, δ_a, and δ_s

According to Eq. (30), the $\delta^{13}C$ of soil-respired CO_2 (δ_ϕ) must also be estimated. This value differs from soil CO_2 (δ_s) by both the 4.4‰ diffusional fractionation between ^{13}C and ^{12}C (Craig, 1953; Cerling et al., 1991b) and the relative input of heavy δ_a. The $\delta^{13}C$ of soil organic matter (δ_{om}) appears roughly equal to its associated δ_ϕ (Cerling, 1992b), and can be taken as a direct proxy (Cerling, 1992b; Mora et al., 1991, 1996). It is possible, however, for differential decomposition, burial diagenesis, or contamination by modern organic matter to jeopardize this equality (Ekart et al., 1999). It is important to measure δ_{om} at each site, and not assume a constant value (e.g., −24‰), because excursions occur in the geologic record (Bocherens et al., 1993; Jones, 1994). Accounting for δ_{om} eliminates the argument that C_4 plants or other unusually ^{13}C-enriched organic matter is the cause for heavy δ_{cc} values, not elevated PCO_2 (Wright and Vanstone, 1991, 1992). Unfortunately, organic matter is often rare in well-aerated soils pertinent to this method (Cerling, 1991, 1999; Mora and Driese, 1999), and some studies simply apply today's mean δ_{om} for C_3 plants to their fossil sites (e.g., Lee, 1999).

The $\delta^{13}C$ of the atmosphere (δ_a) is required by the model, but is one of the least sensitive variables (Cerling, 1992b). Typically, values are derived from the marine carbonate record (δ_{occ}) (e.g., Veizer et al., 1999), assuming a constant fractionation and ocean–atmosphere equilibrium (but see Section 3.5). The assumption of equilibrium may not be valid during intervals of rapid global change such as the P–E boundary (Ekart et al., 1999). δ_a has in turn been used as a δ_{om} proxy. Ekart et al. (1999) used a smoothed version of the δ_{occ} curve of Veizer et al. (1999) to infer δ_a, and then assumed a constant fractionation of 18‰ between the atmosphere and organic matter (Δ_{a-om}). While this procedure was required to compare studies that had not measured δ_{om} with those that had, it nonetheless potentially introduces error, both because Δ_{a-om} may not be constant and the smoothed Veizer et al. (1999) curve does not accommodate for short-term δ_a excursions. In addition, plants growing in the seasonably dry to semi-arid regions conducive to pedogenic carbonate

formation are likely to be water stressed, which may reduce Δ_{a-om}. Calculating δ_{om} from δ_a also greatly increases the sensitivity of the model to δ_a (Fig. 6). This may be important for times where δ_{occ} is not well constrained, such as the Permo-Carboniferous. PCO_2 estimates of Ekart et al. (1999) during this interval decrease by 700 to 2500 ppmV when δ_{occ} values from Popp et al. (1986) are used instead of Veizer et al. (1999) (Berner, unpublished data). When possible, δ_{om} should always be measured directly.

The last parameter required to calculate PCO_2 is the $\delta^{13}C$ of the soil CO_2 (δ_s). As discussed above (Section 4.2), since equilibrium is common between δ_s and δ_{cc}, and no other soil component significantly contributes to δ_{cc}, the $\delta^{13}C$ of pedogenic carbonate is used as a proxy. This conversion involves a temperature-dependent fractionation (Eq. (18)), and so soil temperature must be estimated. This variable is not well known, as it depends on air temperature, time of year of carbonate formation, soil texture, and depth in profile. Seasonal temperature fluctuations are dampened in soils at depth, and most pedogenic carbonates form in the low-to-mid-latitudes. An estimate of 25°C is commonly used (Cerling, 1991; Mora et al., 1996; Ekart et al., 1999); however, one could expect considerable variation. Calculations of PCO_2 based on soil temperatures of 20°C versus 30°C can differ by 700 to 1500 ppmV (Cerling, 1999; Ekart et al., 1999).

4.5. C_4 plants

The δ_{om} of C_4 plants is enriched $\approx$14‰ relative to C_3 plants, having a modern mean value of ≈ -12.5‰ (Deines, 1980). This large isotopic difference is reflected in δ_{cc}, and reinforces the need to measure coexisting δ_{om} (Cerling, 1992a,b). If δ_{om} values indicative of C_4 vegetation are found, however, such sites should not be used for estimating paleo-CO_2. The $\delta^{13}C$ gradient between δ_a and C_4-dominated δ_ϕ (ca. 6‰) is much smaller than that between δ_a and C_3-dominated δ_ϕ (ca. 20‰), and thus the precision of PCO_2 estimates based on C_4-dominated sites is much poorer (Cerling, 1984; Fig. 7). Evidence for C_4 plants in pre-Neogene deposits is sparse (Cerling, 1991; but see Bocherens et al., 1993; Jones, 1994), and so is not a critical issue for older sites.

4.6. Choosing appropriate paleosols

Substantial literature exists pertaining to identifying paleosols in the field (e.g., Retallack, 1988, 1990). Common characteristics include clayskin-

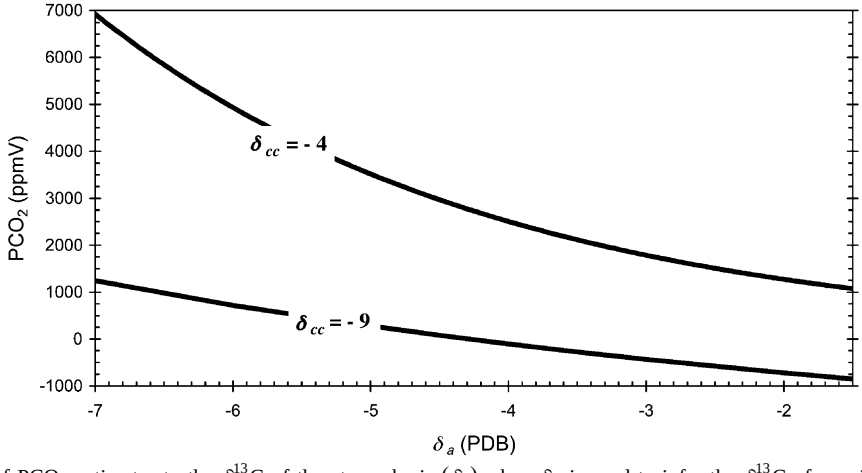

Fig. 6. Sensitivity of PCO_2 estimates to the $\delta^{13}C$ of the atmospheric (δ_a) when δ_a is used to infer the $\delta^{13}C$ of coexisting organic matter (δ_{om}) (e.g., Ekart et al., 1999). The two $\delta^{13}C$ values of pedogenic carbonate (δ_{cc}) span most of the range currently observed in the fossil record. Note that the sensitivity increases with heavier δ_{cc} and lighter δ_a (i.e., at higher PCO_2). Lines drawn from Eqs. (18) and (31) assuming $S(z) = 5000$ ppmV, soil temperature = 25°C, $\Delta_{occ-a} = 8$‰, and $\Delta_{a-om} = 18$‰. Assuming a constant Δ_{occ-a}, differences in published δ_a values for the Permo-Carboniferous exceed 2‰ (see Section 4.4 for discussion).

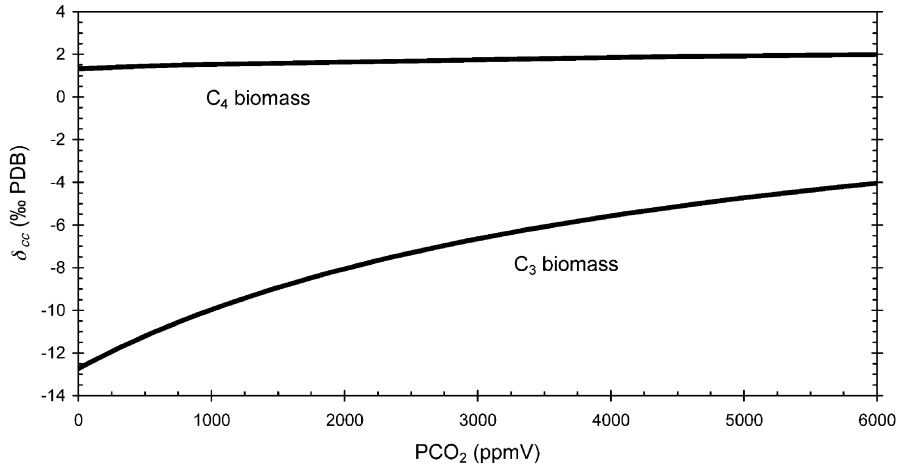

Fig. 7. Difference in sensitivity of PCO_2 estimates between pedogenic carbonate formed in pure C_3 and C_4 biomass systems. Lines drawn from Eq. (31) assuming $S(z) = 4500$ ppmV, $\Delta_{cc-s} = 9.0‰$, $\delta_a = -6.5‰$, and $\delta_\phi = -26\%$ and $-12‰$ for C_3 and C_4 biomass, respectively.

bounded peds, root traces, and evidence of bioturbation (Cerling, 1992a, 1999). Further analysis is required, however, to determine if a given paleosol is appropriate for this method. Although analyses of δ_{cc} from modern soils show little input from detrital carbonate, even for soil profiles developed on carbonate parent material (Quade et al., 1989), it is wise to avoid such soils (Cerling, 1984; Ekart et al., 1999). This is particularly important for paleosols lacking well-developed leached horizons above the pedogenic carbonates, as the δ_s in such soils are often influenced by detrital carbonate (Cerling, 1992a, 1999). Likewise, potential paleosols resting on marine or lacustrine carbonates should be avoided (Mora et al., 1991; Driese et al., 1992; Cerling, 1999; Ekart et al., 1999). Groundwater calcretes are always to be avoided, as they do not form in a diffusion-dominated system. Such soils may show signs of gleying, or contain massive carbonate deposits, but can be difficult to distinguish from pedogenic carbonates formed in unsaturated zones (Cerling, 1999).

Carbonates that formed in soils with little biological activity (e.g., before the Devonian colonization of vascular land plants) should be treated with caution, since their associated respiration rates were undoubtedly very low (Mora et al., 1991; Ekart et al., 1999), leading to inflated estimates of PCO_2. In addition, under such conditions carbonates are much more likely to form abiotically (Mora et al., 1991; Mora and Driese, 1999).

As discussed above (Section 4.2), it is crucial for soils with moderate to high respiration rates to measure δ_{cc} from > 50 cm depth. Analyzing soils at too shallow of a depth will lead to overestimation of PCO_2. Mora et al. (1996) found that in paleo-vertisols, which seasonally formed deep cracks, the δ_{cc} of nodules were consistently heavier than the δ_{cc} of rhizoliths deeper in the profile. This may also highlight the need to sample deeper in vertic paleosols due to their associated greater penetration of atmospheric CO_2 (Mora and Driese, 1999).

Burial diagenesis can potentially alter the δ_{cc} signature. Most studies find no evidence for burial diagenesis, however, even in recrystallized carbonates with large intra-site $\delta^{18}O$ variability (Cerling, 1991; Mora et al., 1996). Nevertheless, micritic carbonate in the form of distinct nodules or rhizoliths is preferable. Veins, coalballs, septarian nodules, and radiating crystals are to be avoided (Ekart et al., 1999).

4.7. Goethite method

An independent PCO_2 proxy has been developed involving trace pedogenic carbonates contained within goethites ($Fe(CO_3)OH$) (Yapp and Poths, 1992, 1996). In brief, the concentration and $\delta^{13}C$ of

this goethite is a function of C_s^* and δ_s, respectively, so that the atmosphere–goethite–organic matter system can be modeled as simple mixing between the two end members (Yapp and Poths, 1992):

$$\delta_g = \left(\delta_{g(a)} - \delta_{g(om)}\right) X_a/X + \delta_{g(om)} \quad (32)$$

where $\delta_g = \delta^{13}C$ of goethite, $\delta_{g(a)}$ and $\delta_{g(om)}$ = the theoretical δ_g if only influenced by the atmosphere and organic matter, respectively, X = mole fraction of $Fe(CO_3)OH$ in the goethite, and X_a = the theoretical X if only influenced by the atmosphere.

Thus, in a preserved soil profile, δ_g will decrease and X increase with depth, and they are inversely related to one another (Yapp and Poths, 1992). This relationship is insensitive to variations in soil productivity. If one plots $1/X$ vs. δ_g, the slope term $([\delta_{g(a)} - \delta_{g(om)}]\ X_a)$ is related to PCO_2. If multiple measurements within a given profile are possible, the intercept term should be $\delta_{g(om)}$ (Yapp and Poths, 1992). Multiple measurements are often not possible, however, in which case the $\delta^{13}C$ of coexisting organic matter can be taken as a direct estimate (Yapp and Poths, 1996). As in the analogous case of Ekart et al. (1999), $\delta_{g(a)} - \delta_{g(om)}$ is assumed invariant through time (Yapp and Poths (1996) use 16‰), allowing for the calculation of X_a. As discussed above (Section 4.4), this assumption can be dangerous. PCO_2, in turn, is related to X_a via Henry's law.

Although this model is rather sensitive to temperature (Yapp and Poths, 1992), published error estimates for PCO_2 ($\pm \sim 1200$ ppmV) only account for variability in $\delta_{g(om)}$ (Yapp and Poths, 1996). As with the model of Cerling (1984, 1991), carbonate-containing soils that developed without a strong biological component (e.g., before the rise of vascular land plants) are prone to contain a non-biogenic fraction, and should be treated carefully.

4.8. Summary

In the absence of C_4 plants, $S(z)$, soil temperature, and PCO_2 are the most sensitive variables in Cerling's model (Cerling, 1991, 1999). Since soil temperature and, in particular, $S(z)$ are not well constrained, it is advisable to include as many soils from geographically diverse sites as possible (Cerling, 1991, 1992; Mora and Driese, 1999). When PCO_2 is low (e.g., $< 10\%$ of $S(z)$), its influence on C_s^* is small, leading to imprecise PCO_2 estimates (Cerling, 1992b). For example, Ekart et al. (1999) estimated PCO_2 from 15 modern soils to be 433 ± 385 ppmV (1σ). Thus, this proxy should not be relied upon when $PCO_2 < \sim 1000$ ppmV. This model also loses precision at high PCO_2 (see Fig. 5), but the rate of loss is less than the other proxies, and should be the proxy of choice when PCO_2 is high ($> \sim 1500$ ppmV). The temporal range of this method also exceeds the other proxies, and should yield reasonable estimates of PCO_2 (± 500 to 1000 ppmV) back to the Devonian, the time of rapid vascular land plant colonization. Pre-Devonian estimates should be considered carefully since terrestrial biological productivity was undoubtedly low.

Unfortunately, the temporal resolution of this method is the poorest of the proxies described here. Pedogenic carbonates typically form on the timescale of 10^3–10^4 years (Cerling, 1984, 1999), which should be considered the upper limit of the method's temporal resolution. Studies wishing to quantify PCO_2 over shorter time intervals should use other proxies. In addition, this proxy should not be used during intervals with sharp isotopic excursions due to potential disequilibria among the isotopic reservoirs (Ekart et al., 1999).

5. Stomatal density and stomatal index

Terrestrial plants obtain CO_2 from the atmosphere for growth, and thus necessarily lose water vapor to an unsaturated atmosphere. The classical dilemma between carbon acquisition and water loss results in the concept of plant water-use efficiency (WUE), which can be defined in a number of different ways. In the short-term of minutes, WUE is calculated as the ratio of assimilation of CO_2 by photosynthesis to loss of water by transpiration (Stanhill, 1986), described by:

$$\mathrm{WUE} = \frac{\dfrac{g_s \times (p_a - p_i)}{1.6 \times P}}{\dfrac{g_s \times (e_i - e_a)}{P}} = \frac{A}{E} \quad (33)$$

where g_s is the stomatal conductance to water vapor, which is 1.6 times lower when considered as a conductance to CO_2, p_a and e_a are the partial pressures of CO_2 and water vapor, respectively, in the

air outside the leaf, p_i and e_i are the partial pressures of CO_2 and water vapor, respectively, in the leaf air spaces and P is the atmospheric pressure. This definition simplifies to:

$$\mathrm{WUE} = \frac{p_a - p_i}{1.6 \times (e_i - e_a)} \quad (34)$$

and emphasizes the importance of stomatal behavior and morphology on the bi-directional control of CO_2 and water vapor fluxes from the leaf. It should be noted in passing that timescales are of crucial importance to plant WUE. On the longer timescale of a day, net assimilation will be less than expected by just integrating assimilation rates during the whole day, because respiratory loss of CO_2 by non-photosynthetic organs, and by leaves in darkness, must be accounted for (Farquhar et al., 1982; Farquhar and Richards, 1984). In addition, water loss may occur through the leaf cuticle (Jones, 1992), a feature that is rarely measured. A more complete definition of WUE is therefore given by:

$$\mathrm{WUE} = \frac{(p_a - p_i) \times (1 - \varphi_r)}{1.6 \times (e_i - e_a) \times (1 + \varphi_w)} \quad (35)$$

where φ_r is the fraction of assimilates respired away by the plant and the term $(1 + \varphi_w)$ allows for transpiration through the cuticle.

The WUE of plants over an entire growing season includes plant respiratory carbon losses through maintenance and synthetic respiration (Jones, 1992) and whole-canopy transpiration calculated from growth analyses:

$$\mathrm{WUE} = \frac{k \times \dfrac{W_e - W_0}{t_e - t_0}}{\int E \mathrm{d}t} \quad (36)$$

where W_0 and W_e are the total dry weights of the plant at the beginning, t_0, and end, t_e, of the growing season, $\int E\mathrm{d}t$ is the sum of daily transpiration and k converts changes in dry matter to CO_2 equivalents. This version of WUE is under variable control by stomatal behavior, depending on the coupling of the canopy with the over-lying air (Jarvis and McNaugthon, 1985).

Plant WUE, as defined in timescales of minutes (Eqs. (34) and (35)), and for whole growing seasons (Eq. (36)), has been correlated with leaf stomatal density (SD) at ambient CO_2 (Beerling and Woodward, 1996a), but plants tend to optimize carbon gain per unit of water loss (i.e., WUE) through the fine control offered by regulating of stomatal opening and closing (Cowan, 1977). In a CO_2-rich atmosphere, leaf WUE increases because CO_2 induced partial stomatal closure reduces water vapor losses without reducing the CO_2-related stimulation of photosynthesis (Morison, 1985). An additional improvement in WUE is possible in an elevated CO_2 atmosphere by reducing the number of stomatal pores (stomatal density, SD) on the leaf surface (Woodward, 1987; Woodward and Bazzaz, 1988). Changes in SD can have an important effect on plant fitness by influencing the growth response of whole plants (Kundu and Tigerstedt, 1999; Hovenden and Schimanski, 2000). Woodward (1987) and Woodward and Bazzaz (1988) demonstrated that atmospheric CO_2 can regulate stomatal formation (Beerling and Chaloner, 1992) and subsequent studies have shown the inverse relationship between stomatal density (SD) and PCO_2 to be widespread across different taxonomic groups (Beerling and Woodward, 1996b) pointing to its potential to offer a plant-based paleo-CO_2 sensor using fossil leaves that extends back through geological time. We emphasize that at the present the underlying genetic mechanism(s) linking CO_2 and SD remains to be identified and so the relationship must be regarded as correlative, not causative.

This section describes important considerations regarding the use of stomatal measurements on fossil leaves to detect paleo-CO_2 signals. For details of fossil leaf cuticle preparation, and methods for standardizing stomatal counts made on leaf surfaces, etc., see Jones and Rowe (1999).

5.1. The concept and use of stomatal index

To interpret paleo-CO_2 signals from fossil leaves, there is need to control for other features of the environment that might influence their stomatal characters (Beerling, 1999). Given that plants tends to optimize their WUE, it follows that water stress would be expected to reduce transpirational water losses, and this is usually brought about through partial stomatal closure in response to drought (e.g., Clifford et al., 1995). It is interesting to note that, paradoxically, SD typically increases under

droughted conditions (Salisbury, 1927; Beerling, 1999; see Tichá, 1982; Royer, 2001 for reviews) because of a reduction in epidermal cell size causing the stomata to be packed closer together. However, under these circumstances, the stomata are nearly closed and the leaf angle relative to the sun is lower, both of which reduce transpiration water losses.

Salisbury (1927) introduced the concept of stomatal index (SI) to remove the effects of drought, calculated as follows:

$$\mathrm{SI}(\%) = \frac{\mathrm{SD}}{\mathrm{SD} + \mathrm{ED}} \times 100 \quad (37)$$

where SD and ED are, respectively, stomatal density and epidermal cell density. Eq. (37) shows that effectively SI is the proportion of epidermal cells that are stomata (where stomata are defined as the stomatal pore and two flanking guard cells). It is therefore independent of epidermal cell size and measures stomatal initiation and development, and is not affected by subsequent cell expansion. Unlike CO_2 (Woodward, 1987; Woodward and Bazzaz, 1988), there is no experimental data demonstrating that water stress influences stomatal initiation (Salisbury, 1927; Sharma and Dunn, 1968, 1969; Estiarte et al., 1994; Clifford et al., 1995).

A recent review of the effects of irradiance, temperature, vapor pressure deficit and water supply on leaf SD and SI concluded that SI has the fortuitous property of being relatively insensitive to all of these but sensitive to atmospheric CO_2 levels, whereas SD can be influenced by each factor separately or in combination (Beerling, 1999). Such considerations clearly indicate that SI rather than SD should be more secure for interpreting paleo-CO_2 variations from fossils. We recognize, however, that epidermal cells can become difficult or impossible to accurately count on poorly preserved fossil cuticles and this in turn requires the use of SD, but with a suitable measure of caution (Beerling et al., 1993; McElwain and Chaloner, 1996).

An important and often over-looked consideration in the relationship between SD/SI and CO_2 is what stomatal development/initiation is responding to. Careful experimental work has shown that plants have the capacity to respond to a reduction in the partial pressure of CO_2 by an increase in leaf SI (Woodward and Bazzaz, 1988). The response, though, is insensitive to changes in the mole fraction of CO_2 (Woodward and Bazzaz, 1988), indicating that the mechanism controlling SI and SD is sensitive to CO_2 partial pressure and not mole fraction (or concentration). Since CO_2 partial pressure falls with increasing altitude, but mole fraction is constant (Gale, 1972), these experimental observations largely explain the general trend of increasing SD of trees and shrubs with altitude (Körner et al., 1986; Woodward, 1986). From this, therefore, it follows that fossil leaves showing changes in SD/SI though time are actually recording ancient variations in atmospheric CO_2 partial pressure. For leaves obtained from sites at altitudes close to sea level, the partial pressure of CO_2 is approximately equivalent to CO_2 concentration; quantitative CO_2 partial pressure reconstructions from SD/SI measurements can therefore be readily converted to units of CO_2 concentration. However, for paleo-CO_2 reconstructions using fossils from sites at significant altitude, such a conversion requires the difficult-to-test assumption that total atmospheric pressure has not changed (cf. Rundgren and Beerling, 1999). Clearly, it is advisable to control for paleoaltitude during the design of investigations aiming to reconstruct paleo-CO_2 variations with this technique.

5.2. Canopy-scale considerations

Due to canopy photosynthesis and plant and soil respiration, the CO_2 concentration experienced by leaves within a canopy can deviate from the global ambient value (Bazzaz and Williams, 1991; Buchmann et al., 1996). This, in turn, may introduce bias in PCO_2 estimates from the SD/SI measurements made on fossil leaves if derived from a dense closed-canopy where the PCO_2 values at the time of stomatal development in the leaf were very different from ambient. Atmospheric data from Harvard Forest in north central Massachusetts, USA, indicate that CO_2 concentration differences between the ambient atmosphere and close to the ground surface (4.5 m) can be as large as 35 ppmV, especially during the summer when soil and plant respiration rates are high (Fig. 8). However, since bud formation and bud-burst by deciduous trees typically occurs in the spring and fall when CO_2 differences between the ambient atmosphere and canopy are < 10 ppmV

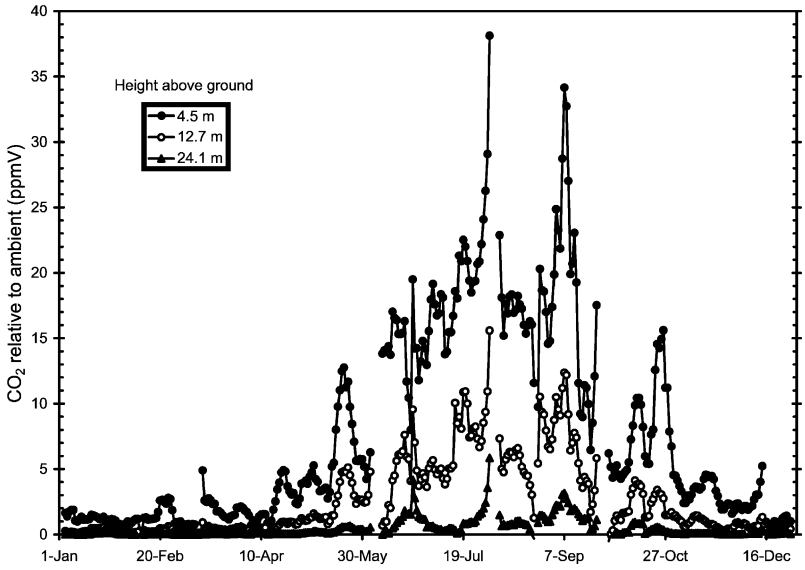

Fig. 8. Canopy CO_2 relative to ambient CO_2 for four heights within a tree canopy in 1996. Canopy height is ca. 24 m. Ordinate represents 7-day running average of daily averages of hourly measurements at each height ($n = 5311$ for each height). Measurements at 29.0 m height taken as ambient value (mean for time interval at this height = 370 ppmV). Raw data available at http://www.as.harvard.edu/chemistry/hf/profile/profile.html, and used with permission of S. Wofsy.

(Fig. 8), this effect by itself is unlikely to strongly bias paleo-CO_2 trends.

For tropical forests, it is important to note that the potential for a forest canopy to become uncoupled from the over-lying atmosphere, and therefore alter the local CO_2 environment, is strongly dependent upon the regional meteorology and geographical location (cf. Grace et al., 1995). Leaf life spans and primary production in tropical evergreen trees tends to occur continuously so that a single canopy comprises of a range of cohorts (e.g., Reich et al., 1991; Clark et al., 1992; Williams-Linera, 1997) that potentially developed at different CO_2 concentrations. This suggests that the use of fossil leaves from stratified ancient Mesozoic and Tertiary tropical forests for paleo-CO_2 signals may be more susceptible to errors arising from within canopy PCO_2 fluctuations; for tropical Amazonian forests, within canopy PCO_2 values are 30% higher than the global value (Grace et al., 1995).

A more important effect of canopy development is the logarithmic attenuation of irradiance with canopy depth, described by Beers' Law as:

$$I = I_0 \times e^{-kL} \quad (38)$$

where I_0 is the photosynthetically active irradiance incident on a canopy, I is the irradiance beneath a leaf area index L, and k is the extinction coefficient for irradiance (typically 0.5). This effect results in the development of so-called sun and shade leaves (Givnish, 1988) with differing SD values; SI values remain largely conservative (Salisbury, 1927; Kürschner, 1997; Wagner, 1998). It might be envisaged therefore that SD (and possibly SI) determinations from fossil leaf assemblages constituting a mixture of sun and shade leaves might introduce a bias resulting from this effect (Poole et al., 1996). There is some hope that such a bias is minimized in the fossil record. Studies on the transport processes responsible for sorting leaf material prior to fossilization indicate a preferential selection of sun morphotypes (Spicer, 1981) and in this context, careful consideration of the depositional environment is required.

It is interesting to speculate that these two features (CO_2 and irradiance) of the environment altered by canopy development might be expected to lead to evolutionary differences in the absolute stomatal density of understory herbs and trees, as proposed nearly 70 years ago by Salisbury (1927). A

re-analysis of his data, accounting for the effects of taxonomic relatedness, revealed that in fact tree species typically have higher stomatal densities than herbaceous species (Kelly and Beerling, 1995), although as expected marginal herbs had significantly higher stomatal densities than understory herbs. In terms of their responsiveness to CO_2 increases, both recent historical and experimental, no strong correlations between stomatal density and growth form (woody vs. non-woody; trees vs. shrubs), habitat (cool vs. warm), or taxonomic relatedness have been reported (Woodward and Kelly, 1995; Beerling and Kelly, 1997).

5.3. Temporal sensitivity of stomatal responses to CO_2 change

The inverse relationship between SI and atmospheric CO_2 has been reported as non-linear at CO_2 concentrations above ambient (Woodward and Bazzaz, 1988; Kürschner et al., 1997), although between the range 250–370 ppmV most species typically show a linear response (Fig. 9). Indeed, a literature survey of 65 SI responses (from a pool of 35 species) to experimental CO_2 enrichment (usually $2\times$ ambient) reported that 29% of cases showed a reduction, with 66% showing no significant response, and the remaining 5% showing an increase (Royer, 2001). SD responses followed a similar pattern. In these studies, the median length of exposure to an instantaneous step increase in atmospheric CO_2 concentration was 45 days. However, analysis of the response of SD and SI on fossil leaves spanning the last 400 m.y. to CO_2 concentrations above ambient, as determined from independent PCO_2 proxies and long-term geochemical models, indicates an inverse linear relationship (Fig. 10) (Beerling and Woodward, 1997; Royer, 2001). The data from fossils therefore intimate that the apparent 'ceiling' CO_2 concentration to which SD/SI respond is mutable and that given sufficient time to adapt, plants have the capacity to respond to above ambient CO_2 concentrations. The implication is that the stomatal method of paleo-CO_2 estimation could potentially detect CO_2 increases above ambient despite the apparent non-linear response shown by modern genotypes.

The reason for the apparent insensitivity in over half the species studied to date in short-duration experiments is not known, but may be related to the 'ceiling' to which modern genotypes have become adapted over the past ~ 2 m.y. of glacial–interglacial CO_2 fluctuations (Woodward, 1987; Beerling and Chaloner, 1993). If the linkage between PCO_2 and stomatal initiation is genetically based, it might

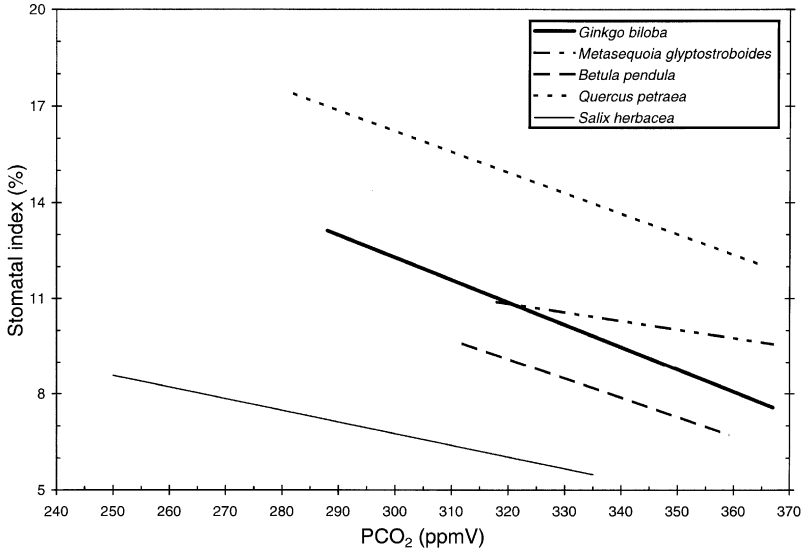

Fig. 9. Stomatal index response of five species to PCO_2. Data compiled from herbarium sheets and altitudinal transects. Sources are as follows: *Ginkgo biloba* and *Metasequoia glyptostroboides* (Royer, unpublished data); *Betula pendula* (Wagner et al., 1996); *Quercus petraea* (Kürschner et al., 1996); *Salix herbacea* (Rundgren and Beerling, 1999).

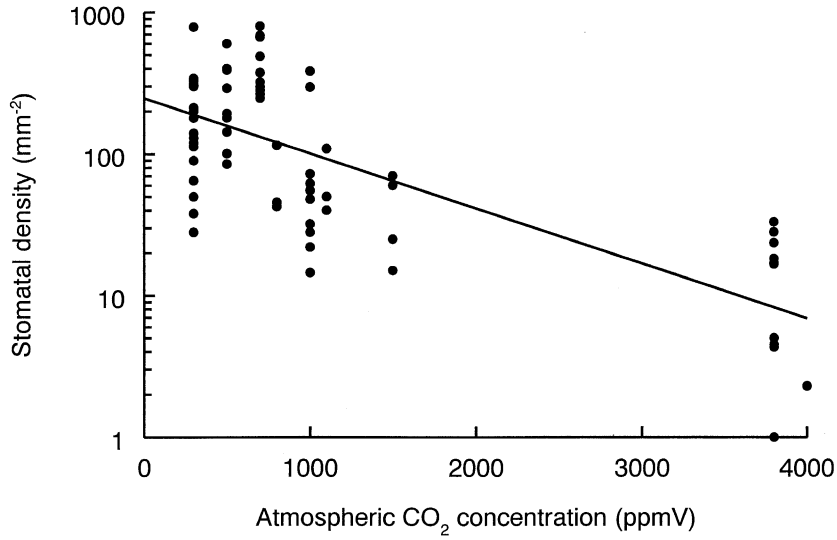

Fig. 10. Response of stomatal density measured on fossil leaves/axes to atmospheric CO_2 variations over the Phanerozoic ($r = 0.74$). Redrawn from Beerling and Woodward (1997) with additional data from Cleal et al. (1999) and Edwards (1998). CO_2 data from Berner (1994).

involve a time lag. The possibility of a genetic basis is intimated by transplant experiments with the upland grass *Nardus stricta* (Woodward and Bazzaz, 1988) and analysis of plants growing near natural high CO_2 springs for many generations (Beerling and Woodward, 1997; Bettarini et al., 1997, 1998; Fernández et al., 1998; Paoletti et al., 1998; Tognetti et al., 2000). In a reciprocal transplant experiment, plants of the herbaceous species *Tussilgao farfara* collected close to a geothermal spring in Italy, known to have grown under elevated CO_2 concentrations for many decades, and those from control ambient CO_2 sites, were grown in controlled environments at ambient (350 ppmV) and elevated (700 ppmV) CO_2 partial pressures for two years (Beerling and Woodward, 1997). The results indicated greater reductions in SI under full irradiance conditions by plants from the high CO_2 source, compared to those from the ambient CO_2 source, providing some evidence for genetic adaptation between different plant populations. The response is not, however, seen universally in plants from high CO_2 springs (Bettarini et al., 1998), although in an extreme case, plants of *Spatiphylum cannifolium* and *Bauhinia multinervia* growing at CO_2 concentrations of up to 27,000–35,000 ppmV in a natural cold CO_2 spring in Venezuela were reported to have lower SI values by 70–80% compared to their ambient CO_2 grown counter parts (Fernández et al., 1998).

Whatever the mechanism(s), we note that the unknown duration of exposure required for a plant to adjust its SD/SI value to a high CO_2 regime would appear to define the stomatal paleo-CO_2 method's temporal resolution. For most studies on fossil plants encompassing tens of thousands to millions of years, and therefore many generations of even long-lived trees, it seems reasonable to assume any genetically determined 'ceiling' could be altered.

A further important issue relating to this method is the strength of response, i.e., the magnitude of SI change for a given unit of CO_2 change. Two analyses on a life form basis have concluded that the degree of reduction in stomatal density to CO_2 enrichment increases with the initial stomatal density (Woodward and Kelly, 1995; Beerling and Kelly, 1997), defined by the relationship:

$$SD_E = SD_A - \exp\left(178 \times \ln\left(SD_A\right)^k\right) \quad (39)$$

where SD_A and SD_E are the stomatal densities at ambient and elevated CO_2 concentrations, respectively, and k is the slope of the major axis least squares regression resulting from independent contrasts (see Woodward and Kelly, 1995; Beerling and Kelly, 1997). The relationship is presented with the

caveat that it was derived mainly from short-term studies, with a few samples from studies spanning decades to centuries. As yet, there are insufficient data for similar analyses on SI responses.

The response of SD predicted by Eq. (39) is shown graphically in Fig. 11 for three cases: (1) the SD change predicted from analysis of results from herbarium studies and CO_2 enrichment experiments ($k = 0.348$), (2) the change if only results from experimental CO_2 enrichment studies are included ($k = 0.417$) (Woodward and Kelly, 1995) and (3) the change predicted from a study of SD changes in

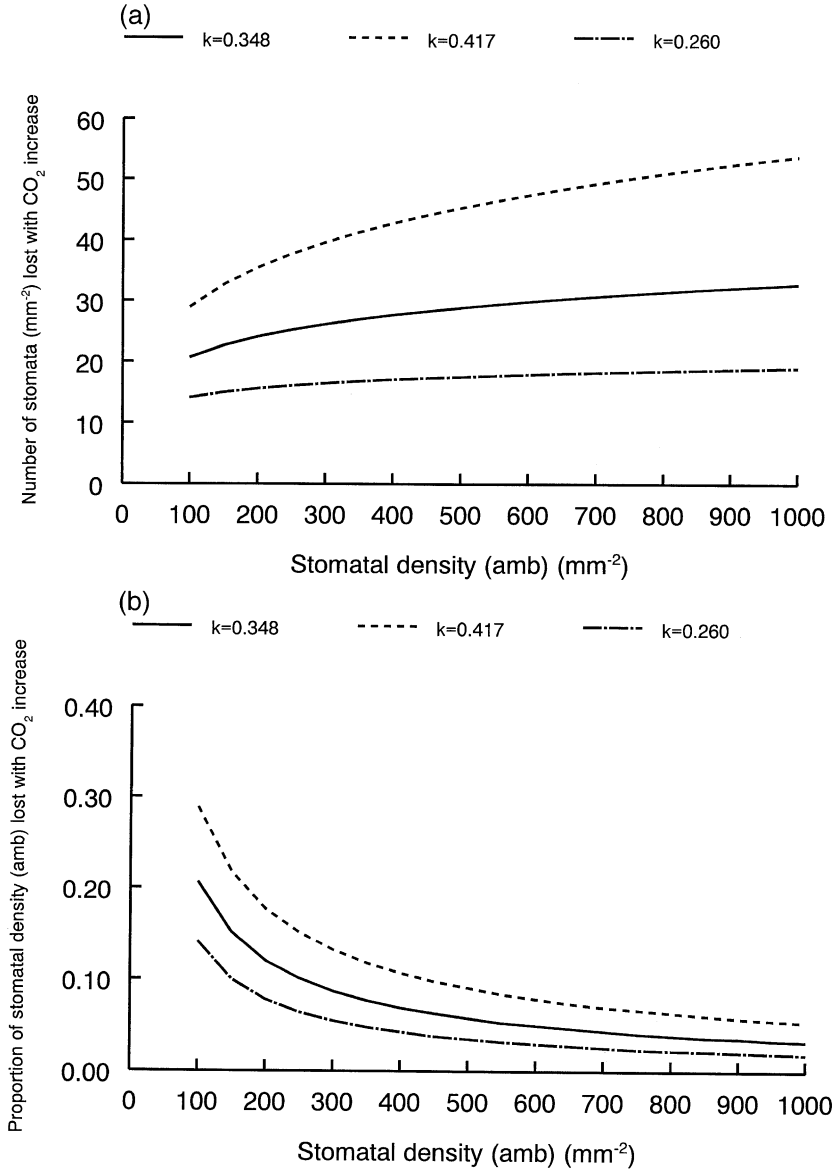

Fig. 11. Generalized relationship between the initial stomatal density of a leaf grown at ambient CO_2 (amb) and (a) the loss of stomata from that leaf after growth with CO_2 enrichment and (b) expressed as the proportion of stomata lost at high CO_2. Calculated from Eq. (39) based on analyses of herbarium and CO_2 enrichment studies ($k = 0.348$), CO_2 enrichment studies only ($k = 0.417$) and the response of a woodland flora to the past 70 years of CO_2 increase ($k = 0.260$).

British woodlands to the past 70 years of CO_2 increase ($k = 0.26$) (Beerling and Kelly, 1997). It can be seen that across all cases, plants tend to dispense with between 10 and 50 stomata/mm^2 in an elevated CO_2 atmosphere (Fig. 11a), constituting a loss of between 30% and 10% of their original density (Fig. 11b). The relationships imply that there is a maximum number of stomata that can be lost; leaves cannot function effectively without stomata, and this has led to the suggestion that in the short-term response curve that is sigmoidal (van der Burgh et al., 1993; Kürschner et al., 1997). The exceptions to this statement are some amphibious species such as *Littorella uniflora* (Nielsen et al., 1991) and *Lobelia dortmanna* (Pedersen and Sand-Jensen, 1992) that function with no stomata at all.

These responses (Fig. 11) relate to the study of fossil materials because extant groups of plants may have SD/SI values reflecting the atmospheric CO_2 partial pressure at their time of origin (Beerling and Woodward, 1996b). For example, gymnosperm lineages evolved during times of perceived high PCO_2 and in general have low SI values today; consequently this minimizes potential for further reductions in SI above present-day PCO_2. On this basis, we suggest it is important to consider the absolute SD and SI values for a species targeted for study as this gives a likely assessment of its potential sensitivity of paleo-CO_2 change. This suggestion probably holds regardless of duration of exposure because of functional considerations required for effective photosynthetic CO_2 uptake and the generation of a transpiration stream.

5.4. Applications of stomatal method to detection of paleo-CO_2 change

Application of stomatal indices as a PCO_2 proxy involves many fewer assumptions and calculations than the other proxies described here (Sections 3, 4, and 6). One simple approach involves tracking relative temporal trends in SD or SI of a single species (Beerling, 1993; Beerling et al., 1993; van de Water et al., 1994; McElwain et al., 1995; Cleal et al., 1999). Only qualitative trends in PCO_2 can be deduced in this manner. Quantitative paleo-CO_2 reconstructions can be made by establishing an SI–CO_2 relationship with known PCO_2, and then using this 'calibration set' to estimate PCO_2 from the SI of the same species from the fossil record. Standard curves generated in this way have to date been derived from a mixture of herbarium data and data from plants growing across altitudinal gradients (e.g., Rundgren and Beerling, 1999; see Fig. 9). Experimental data could also be used to develop training sets for use with pre-Quaternary fossil leaves but in many cases experimental growth conditions are very different from those experienced by plants in the field and some cross calibration is required, e.g., by comparing the SI values of leaves grown at ambient CO_2 partial pressures experimentally and naturally, before combining the datasets.

A detailed quantitative paleo-reconstruction of changes in the partial pressure of atmospheric CO_2 over the last 9000 ka of the Holocene using fossil leaves of *Salix herbacea* has been made by Rundgren and Beerling (1999). These authors reconstructed CO_2 values from SI measurements made on fossil leaves by developing a modern training set of *Salix herbacea* SI values plotted against reference CO_2 partial pressures that were largely independent of ice core data. Their results (Fig. 12a) closely matched the pattern of changes in atmospheric CO_2 concentration documented from the ice core record (Fig. 12b) (Indermühle et al., 1999b), providing independent support for the notion that small changes in atmospheric CO_2 can be sustained despite the relative stability of the global climatic conditions (Ciais, 1999). This detailed, well-dated study provides the strongest validation for the SI-based CO_2 proxy to date and points the way for obtaining quantitative CO_2 reconstructions for the Cretaceous and Paleogene, if a taxon has a sufficiently long fossil record, and has closely related extant representatives amenable to CO_2-enrichment experiments. There are probably no extant stomata-bearing plant species that extend back to the pre-Cretaceous. Particularly useful though are so called 'living fossil' plants, e.g., *Metasequoia glyptostroboides* and *Ginkgo biloba*, a term coined by Darwin to describe extant taxa belonging to lineages characterized by little or no phenotypic change since the Mesozoic (Beerling, 1998a). One possible problem in using these taxa to reconstruct paleo-CO_2 changes in the past is that the calibration dataset will necessarily have been obtained from herbarium studies and ex-

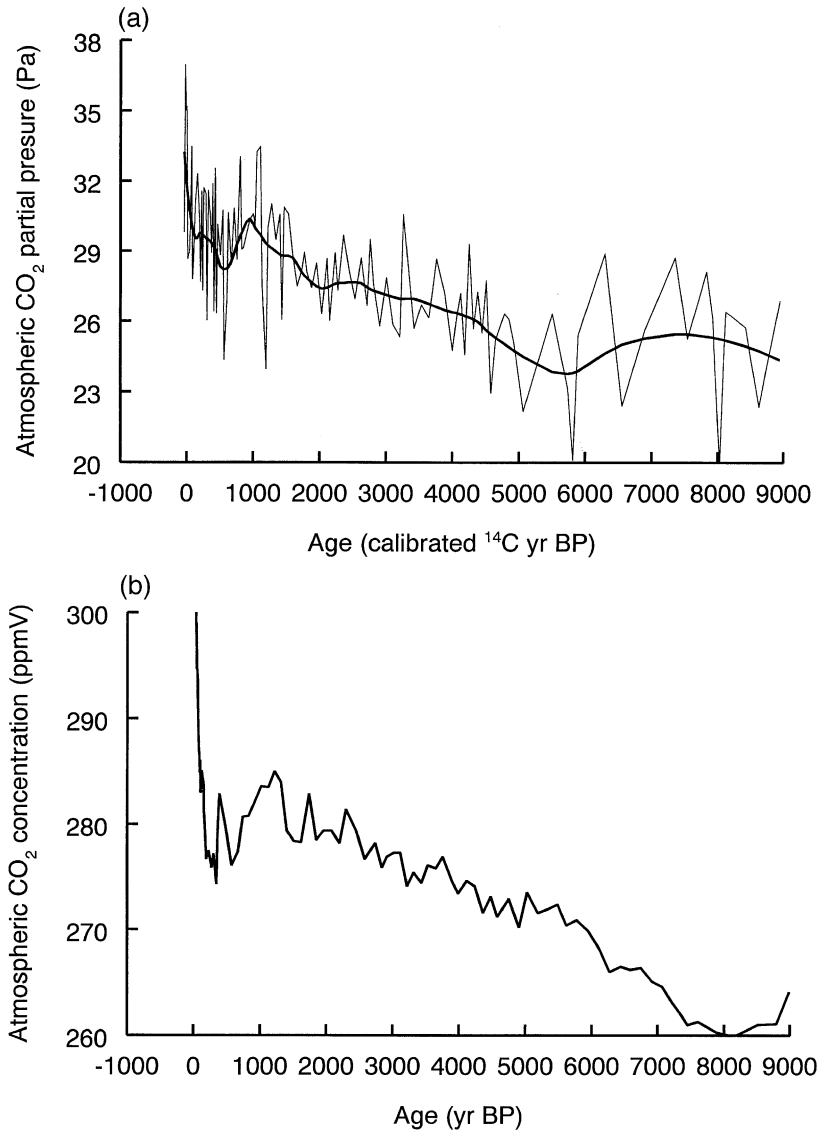

Fig. 12. Holocene reconstructed variations in (a) the partial pressure of atmospheric CO_2 using fossil *Salix herbacea* leaves (after Rundgren and Beerling, 1999) and (b) measurements of atmospheric CO_2 from ice cores (after Indermühle et al., 1999b).

periments with modern genotypes that might show a non-linear response at CO_2 concentrations above ambient. This would limit the ability of the method to accurately reconstruct high PCO_2 values.

Considerable care is required in developing training sets for the purpose of paleo-CO_2 reconstructions, and every effort should be made to obtain materials from a wide range of plants with different genotypes and growing in a variety of different environments (Birks et al., 1999). A recent study of the early Holocene illustrates the difficulties that can arise when these considerations are neglected. Wagner et al. (1999) presented a paleo-CO_2 reconstruction for the early Holocene, using a training set based on historical SI changes from birch (*Betula pubescens, B. pendula*) trees growing at a single site, and the approach yielded values of 240–360 ppmV. These values were consistently 50–100 ppmV higher

than concentrations measured in ice cores (Indermühle et al., 1999a) or reconstructed from fossil *Salix herbacea* leaves (Beerling et al., 1995; Rundgren and Beerling, 1999). Independent studies of the response of SI in *B. pubescens* and *B. pendula* indicate that these taxa are rather insensitive to changes in CO_2 partial pressure with altitude, and increases in the atmospheric CO_2 concentration between 1877 and 1978 (Birks et al., 1999). The discrepancy appears to relate to the construction of a modern calibration dataset without paying sufficient attention to the natural variability of leaf cellular properties of *Betula* trees.

A qualitative approach to estimating changes in paleo-CO_2 in the distant past, independently of the need for calibration datasets, is the use of the stomatal ratio (SR) concept (McElwain and Chaloner, 1995). SR is defined as the ratio of the SI of the Nearest Living Equivalent (NLEs) taxon to the fossil to that of the fossil plant under investigation (McElwain and Chaloner, 1995). NLEs are defined as the nearest ecological and morphological equivalent in modern floras to the fossil plant under consideration. Note that the concept is related to, but distinct from, the Nearest Living Relative approach. Taken as absolute ratios, the picture that emerges from detailed analyses of Devonian, Carboniferous, Permian, Jurassic and Eocene fossil plants, and their NLEs (McElwain and Chaloner, 1995, 1996; McElwain, 1998), is that the SR shows a pattern of response through geological time that mirrors Phanerozoic CO_2 trends predicted from mass balance considerations of the long-term carbon cycle (Fig. 13). In an effort to make the SR method semi-quantitative, calculated values have been linearly scaled with the output of Berner's GEOCARB II model (e.g., an SR value of 2 converts to a PCO_2 of $2\times$ pre-industrial value) (McElwain, 1998). Although useful to a certain extent, the problem with this development is that it fails to provide a method of paleo-CO_2 estimation independent of the models.

5.5. Summary

The precision in PCO_2 estimates via stomatal indices is the highest of any current proxy. When herbarium-based standard curves are inverted, the 95% confidence intervals for PCO_2 predictions fall

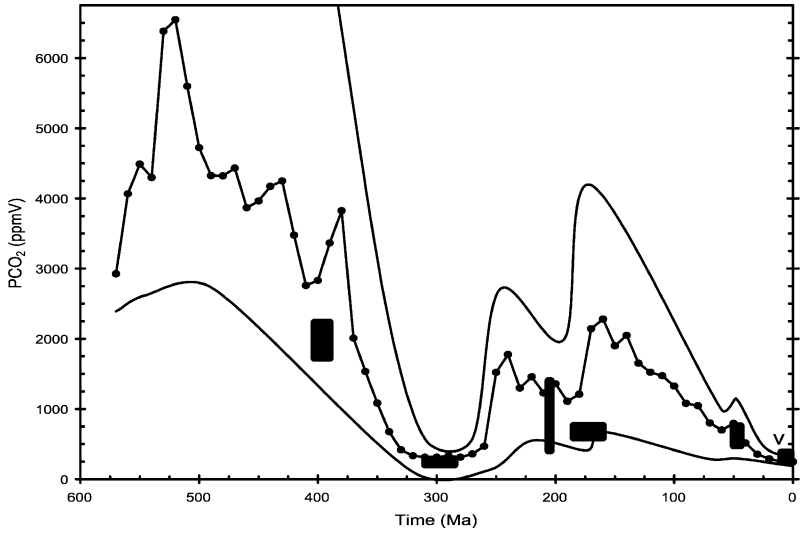

Fig. 13. Comparison of model predictions of atmospheric CO_2 over the Phanerozoic (from Berner and Kothavala, 2001) and stomatal-based estimates. Stomatal ratio data (unmarked filled boxes) from McElwain and Chaloner (1995, 1996) and McElwain (1998). Stomatal index data ('v') from van der Burgh et al. (1993). RCO_2 units (ratio of atmospheric CO_2 in the past relative to the pre-industrial value) of Berner and Kothavala (2001) converted to PCO_2 assuming a time-averaged pre-industrial value of 250 pmmV, which is roughly the mean PCO_2 over at least the last 400 ka (Petit et al., 1999). Middle line represents the "best estimate" predictions of Berner and Kothavala (2001), while the two straddling lines represent error estimates based on sensitivity analyses.

between ±10 and ±40 ppmV (van der Burgh et al., 1993; Kürschner et al., 1996; Rundgren and Beerling, 1999; Wagner et al., 1999; Royer, unpublished data). Thus, this method is preferable for time periods when paleoatmospheric CO_2 was roughly similar to present-day levels. When combined with experimental data, the method can be applied to time periods with elevated PCO_2. At some level of elevated PCO_2, however, SI responses of modern genotypes may have lowered sensitivity (see Section 5.3), resulting in larger error envelopes. This CO_2 saturation level has been observed at around 340 ppmV from some species (Woodward and Bazzaz, 1988), but also frequently to concentrations similar to the phytoplankton proxy (750–1250 ppmV) (Woodward and Kelly, 1995; Kürschner et al., 1997).

This method probably cannot be applied to pre-Cretaceous sites due to its species-specific nature (Section 5.4). For pre-Cretaceous sites, the qualitative stomatal ratio technique of McElwain and Chaloner (1995) can be applied. Relative changes in SD and SI within a given sequence, which also does not require extant species, can be illuminating (e.g., Cleal et al., 1999). The temporal resolution of the SI method can be very high. While multi-million year high-resolution data are not possible as with the phytoplankton method, short-term high-resolution data are widely available. Thus, this method is ideal for resolving potential rapid PCO_2 changes (e.g., K–T boundary, P–E boundary). For example, using the stomatal ratio method, McElwain et al. (1999) documented a large PCO_2 spike across the Triassic–Jurassic boundary at two fossil sites. Additionally, in contrast to the stable isotope-based proxies, the SI method is insensitive to isotopic disequilibria among the biospheric reservoirs, a potential factor during times of rapid global change.

6. $\delta^{11}B$ of marine calcium carbonate

Dissolved boron in the oceans exists primarily as $B(OH)_3$ and $B(OH)_4^-$, and these two species differ in their ratio of the boron isotopes ^{10}B and ^{11}B. Field observations and experimental studies (Hemming and Hanson, 1992; Sanyal et al., 1996) have shown that the uptake of boron into biogenic calcium carbonate records the isotopic composition of $B(OH)_4^-$ with little isotopic discrimination. Because the relative proportions of the two dissolved boron species vary with pH, and the degree of isotopic fractionation between the two species is known, the $^{11}B/^{10}B$ of $B(OH)_4^-$ also varies with pH (Hemming and Hanson, 1992; Sanyal et al., 1996). If the boron incorporated into fossil calcareous organisms faithfully records the isotopic composition of $B(OH)_4^-$ in paleoseawater, it is possible to calculate the value of pH for ancient oceans, once proper corrections for temperature have been made (Spivack et al., 1993; Sanyal et al., 1995, 1996; Palmer et al., 1998; Pearson and Palmer, 1999, 2000). From paleo-pH, making certain assumptions about the behavior of dissolved carbon in seawater, one can calculate paleoatmospheric CO_2 from paleo-pH and an assumed value for total dissolved inorganic carbon (DIC) in seawater. This is the basis for the boron isotopic method for estimating paleo-CO_2. Estimates of CO_2 levels ranging from the Paleocene to the Pleistocene using this method have been made by Pearson and Palmer (1999, 2000).

6.1. Method of calculation

Calculation of the value of pH from boron isotopic data rests on a mass balance expression for boron isotopes and an equilibrium expression for $B(OH)_3$ and $B(OH)_4^-$. For isotopic mass balance:

$$\delta_{B4} X + \delta_{B3}(1 - X) = \delta_{\Sigma B} \quad (40)$$

where $X = [B(OH)_4^-]/([B(OH)_4^-] + [B(OH)_3])$, $\delta_{B4} = \delta^{11}B$ of $B(OH)_4^-$, $\delta_{B3} = \delta^{11}B$ of $B(OH)_3$, $\delta_{\Sigma B} = \delta^{11}B$ of total dissolved boron ($[B(OH)_4^-] + [B(OH)_3]$), and brackets represent molar concentrations. The equilibrium expression for borate chemical equilibrium is (in terms of X):

$$[X][H^+]/[1 - X] = K_B \quad (41)$$

where K_B = the equilibrium constant in seawater. Combining Eqs. (40) and (41) to eliminate (X):

$$[H^+] = K_B(\delta_{\Sigma B} - \delta_{B4})/(\Delta_B - (\delta_{\Sigma B} - \delta_{B4})) \quad (42)$$

where $\Delta_B = \delta_{B3} - \delta_{B4}$ (fractionation between dissolved species). The method, in its simplest form, assumes that $\delta_{\Sigma B}$ and Δ_B are constants, equal to

present values, and that K_B can be calculated for different paleo-temperatures (the small salinity variation for the open ocean should have a minimal effect on K_B). Also, it is assumed that $CaCO_3$ contains only $B(OH)_4^-$ that is taken up with either no fractionation (Hemming and Hanson, 1992; Palmer et al., 1998) or a known constant degree of fractionation Δ_c so that measurement of $\delta^{11}B$ of $CaCO_3$ is equal to $\Delta_c + \delta_{B4}$ (Sanyal et al., 1996).

To convert paleo-pH to paleo-CO_2 further assumptions are necessary. A common assumption is that the total dissolved inorganic carbon (DIC) of the oceans has not changed with time (Pearson and Palmer, 1999). If true, then PCO_2 is calculated from the appropriate equilibrium expression (corrected for changes in temperature) relating DIC, pH, and PCO_2 and using the modern value for DIC. However, if DIC has changed over time, then the calculated result for PCO_2 can be greatly affected. To achieve more constrained PCO_2 estimates, Pearson and Palmer (2000) modeled changes in sea surface alkalinity through time, which can also be used to convert pH to PCO_2. They predicted an overall decrease in alkalinity from 60 Ma to present day. This trend has been independently corroborated using the $\delta^{44}Ca$ of marine carbonates as a proxy for $[Ca^{2+}]$, which should inversely relate to alkalinity (De La Rocha and De Paolo, 2000).

6.2. Problems with the method

Values of K_B and Δ_B are functions of temperature, so that in estimating paleo-pH correction for the effect of changes in temperatures on these parameters needs to be made. This can be done for ancient environments where paleoceanographic data are available (e.g., Palmer et al., 1998; Pearson and Palmer, 1999, 2000). However, a more serious problem arises in assuming that $\delta_{\Sigma B}$ has remained nearly constant over time. Lemarchand et al. (2000) have shown that the boron isotopic composition of the ocean most likely has varied considerably over the Cenozoic due to changes in the inputs and outputs of boron to and from the oceans. For example, they show that the boron isotopic composition of present-day rivers varies by over 40‰ in $\delta^{11}B$. Thus, changes in the relative proportions of riverine input from different sources over millions of years (their estimate of the mean residence time of B in seawater is 14 million years) could alter oceanic B isotope composition to an extent greater than that resulting from variations in pH. Even holding the isotopic composition of riverine input constant, Lemarchand et al. (2000) show that Cenozoic changes in $\delta_{\Sigma B}$ could be as much as 2‰ in 20 million years. A difference of 2‰ is equivalent to a change in pH of 0.3 units (Palmer et al., 1998), which means a change in PCO_2 of a factor of 2 to 4.

Another problem arises from the assumption of the degree of fractionation of isotopes during the incorporation of boron in $CaCO_3$. Since fractionation during biological uptake has been demonstrated to vary among species due to vital effects, it is important to ascertain how this fractionation might vary with different organisms. Hemming and Hanson (1992) found little evidence for fractionation for a variety of modern calcareous organisms, but this was not verified by Vengosh et al. (1991) who found much larger variations. Sanyal et al. (1995, 1996), based on experimental and field studies, found a constant fractionation of about 4‰ for one foram species, *Orbulina universa*, but found no fractionation for another foram, *Globigerinoides sacculifer*. In the paleo-pH studies of Palmer et al. (1998) and Pearson and Palmer (1999, 2000), it is assumed that there was no fractionation for a variety of different foram species; in other words, the boron isotopic composition of calcite represents that for $B(OH)_4^-$ in the original seawater (in the above notation they assume that $\Delta_c = 0$). In the study of Pearson and Palmer (1999), support for this assumption is provided by the finding of essentially the same $\delta^{11}B$ for different foram species from the same depth (temperature) range. However, the variability for forams was found to be greater (up to 4‰) for a larger number of samples in the study by Palmer et al. (1998).

Diagenesis can bring about appreciable changes in the boron isotopic composition of $CaCO_3$ during burial. Spivack and You (1997) have convincingly demonstrated this from the analyses of bulk carbonate in an ODP core from the eastern equatorial Pacific Ocean. Here, they found that the $\delta^{11}B$ of carbonates ranged from -5.5‰ to 23‰ with the most negative values representing a totally recrystallized end member. In the same sediments, interstitial waters showed much less variation in $\delta^{11}B$ with

depth because of diffusional and advectional exchange with seawater.

Finally, there is the problem of calculating paleo-CO_2 from paleo-pH. First of all, one must assume equilibrium of CO_2 between that dissolved in the oceans and that present as a gas in the atmosphere (see Section 3.5). More important, it is not likely that the oceans have exhibited a constant level of DIC over millions of years, as assumed in the calculations of Pearson and Palmer (1999) (but not in those of Pearson and Palmer, 2000). Carbon is continuously supplied to the atmosphere and ocean by degassing from metamorphism and magmatism, and by the weathering of carbonate minerals and organic carbon, and is continuously consumed by the production of carbonate and organic carbon sediments (Berner, 1999). Hence, the total dissolved inorganic carbon load of the ocean could be expected to vary over time.

6.3. Summary

The boron isotope method provides an independent check on other paleoatmospheric CO_2 methods. However, it is based on many assumptions that, if not correct, can lead to incorrect results. Before this method can be put into general use, it will be necessary to gain a better idea of the $\delta^{11}B$ of ancient oceans, how boron isotopes are fractionated during uptake by various calcareous organisms, and how one can estimate the level of dissolved inorganic carbon in ancient oceans.

7. Redox chemistry of marine cerium

Liu and Schmitt (1996) have devised a rather ingenious method, involving many equilibrium steps, for deducing paleo-CO_2 levels from the concentration of cerium in sedimentary rocks. Their method, however, rests upon many assumptions. Among others, these include: (1) the reaction $4Ce^{3+} + O_2 + 4H^+ = 4Ce^{4+} + H_2O$ is at chemical equilibrium at all times; (2) total dissolved Ce in seawater is accounted for almost entirely by carbonate-complexed species; (3) the total dissolved inorganic carbon DIC and alkalinity of seawater remains constant over geological time; (4) the level of dissolved oxygen within the upper 600 m of the oceans does not change with time; (5) the activity coefficient of Ce in sedimentary minerals remains constant over time.

All of these assumptions (and several others not discussed here) have serious problems. Moffett (1990) has shown that Ce oxidation is microbially affected and that the redox couple in seawater is not explained simply by equilibrium with O_2 and H_2O. Cerium is a highly charged trace element (about 10^{-12} M) in seawater and could easily be complexed with many other species (such as dissolved organic matter) other than carbonates. As is stated in the section on the boron isotope method (Section 6.2), it is likely that (DIC) and alkalinity have varied considerably over time. During several times in the geologic past, the average O_2 level in upper portions of the oceans could have varied considerably (e.g., anoxic oceanic events during the Mesozoic). Finally, it is not clear in what mineral form Ce was originally present in any given sediment sample (Liu and Schmidt analyzed carbonates) and what were its solid solution properties; so it is difficult to assume that its thermodynamic behavior in the solid state has been constant over time.

8. Phanerozoic CO_2 trends: a comparison of methods

From this review of paleo-CO_2 proxies, it is clear that different methods have different temporal resolutions (i.e., the amount of time a single sample integrates), and could be usefully viewed in a hierarchical series with the long-term carbon cycle models providing the overarching set of predictions on a timescale of millions of years. Next, paleosol CO_2 proxies provide coverage on a timescale of 10^3–10^4 years (the minimum time required for soil carbonates to form), and these offer a broad crosscheck on the mass balance model results. The two ocean CO_2 proxies, phytoplankton carbon isotopes and boron isotopes, are limited by the resolution of the marine records that depend on factors such as burial rate, productivity, and intensity of bioturbation. A reasonable limit in temporal resolution for organic carbon in pelagic sediments is 10^3–10^4 year (Kennett, 1982). The terrestrial stomatal-based PCO_2 indicator probably offers the best temporal resolution. In this

case, the temporal resolution of pre-Quaternary leaves will typically be limited by the response time for a given species, which can range anywhere between several months to 10^2 year. This gives the following sequence of temporal sensitivity: mass balance < paleosols ≈ phytoplankton = boron isotopes < stomata. This emphasis on timescales is important because for a given method to detect a change in the concentration of atmospheric CO_2, its response time needs to be less than an individual component of the global carbon cycle, i.e., turnover times of organic and inorganic carbon in the oceanic, atmospheric, marine and terrestrial components.

Other important temporal considerations are how well an individual PCO_2 estimate can be dated, and the availability of continuous sequences. In most cases, the errors in absolute dating far exceed temporal resolutions, and so the ability to compare PCO_2 estimates from different localities is diminished. In general, however, marine-based proxies can be better dated than terrestrial-based ones. Temporal trends in PCO_2 are best captured in continuous (or near continuous) sequences. Again, very good sequences exist in marine settings. For example, the average sampling density in Pagani et al.'s (1999a,b) sequence was ~200 k.y., and in some settings it may be possible to sample at or near the single-sample integration time (~10^3–10^4 year). Sequences of paleosols are less common, and generally more temporally discontinuous. Sequences of plant assemblages vary in temporal quality. For example, lacustrine sequences can have annual resolution, but rarely persist for great lengths of time.

Paleo-CO_2 proxies also vary in their precision of PCO_2 estimates. For geochemical models, the precision of PCO_2 predictions can only be assessed via qualitative sensitivity analyses (Section 2.2). In the case of Berner and Kothavala (2001), CO_2 sensitivity ranges from ±75–200 ppmV for the Tertiary to ±1500–3000 ppmV for the early Paleozoic (see Figs. 13–16). The pedogenic carbonate proxy ranges in error from ±400–500 ppmV for the Tertiary to ±500–1000 ppmV for the mid-Paleozoic through Mesozoic (see Fig. 14). PCO_2 error estimates from

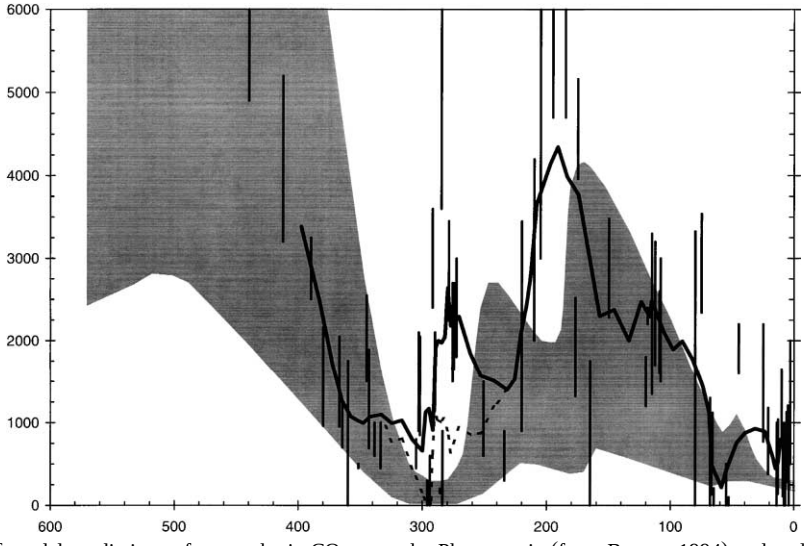

Fig. 14. Comparison of model predictions of atmospheric CO_2 over the Phanerozoic (from Berner, 1994) and pedogenic carbonate-based estimates (including the goethite method). The shaded region represents the error estimates of Berner and Kothavala (2001). RCO_2 units of Berner and Kothavala (2001) converted to PCO_2 as in Fig. 13. Vertical lines represent 78 pedogenic carbonate-based PCO_2 estimates (data from Suchecky et al., 1988; Platt, 1989; Cerling, 1991, 1992a,b; Koch et al., 1992; Muchez et al., 1993; Sinha and Stott, 1994; Andrews et al., 1995; Ghosh et al., 1995; Mora et al., 1996; Yapp and Poths, 1996; Ekart et al., 1999; Elick et al., 1999; Lee, 1999; Lee and Hisada, 1999). The solid line is a five-point running average of the mean PCO_2 of every estimate. This approach smoothes short-term CO_2 fluctuations and is more directly comparable with the model of Berner and Kothavala (2001). The dashed line is a five-point running average incorporating a recalculation of Ekart et al. (1999) data during the late Carboniferous and early Permian using the marine carbonate $\delta^{13}C$ data of Popp et al. (1986) (see Sections 4.4 and 8 for details).

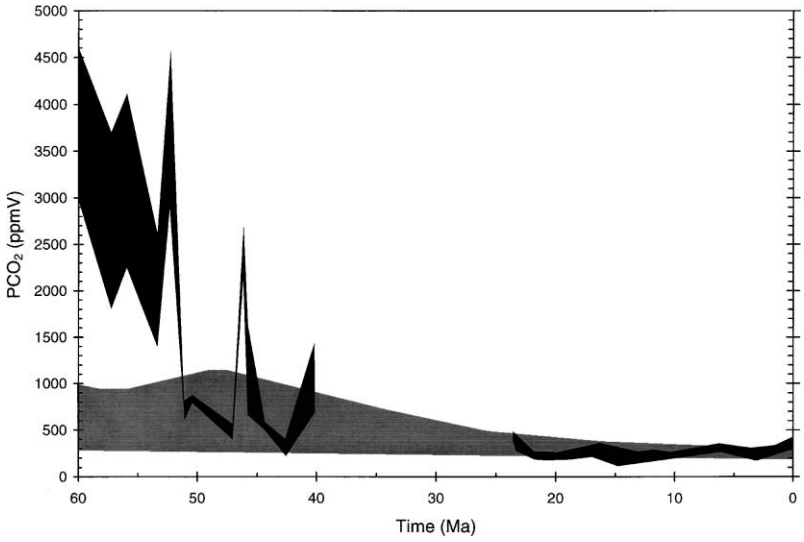

Fig. 15. Comparison of model predictions of atmospheric CO_2 over the last 60 Ma (gray shaded area; from Berner and Kothavala, 2001) and marine δ^{11}B-based estimates (black shaded area; from Pearson and Palmer, 2000). RCO_2 units of Berner and Kothavala (2001) converted to PCO_2 as in Fig. 13.

the δ^{13}C of phytoplankton range from $\pm$25–100 ppmV for the Tertiary to $\pm$150–200 ppmV for the Cretaceous (see Fig. 16). Above $\sim$1000 ppmV, this method loses its sensitivity. For stomatal indices, error estimates for the Tertiary are $\pm$10–40 ppmV (Royer, unpublished data; see Fig. 13). Depending on the plant species chosen, this method's sensitivity to PCO_2 diminishes at some point above 350 ppmV. Additionally, quantitative pre-Cretaceous estimates are probably not possible due to the lack of long-

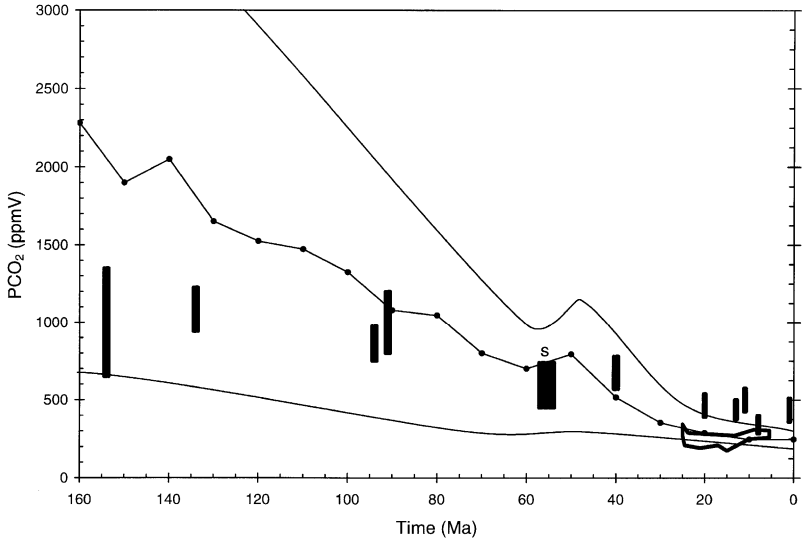

Fig. 16. Comparison of model predictions of atmospheric CO_2 over the last 160 Ma (from Berner and Kothavala, 2001) and marine organic matter δ^{13}C-based estimates. Unmarked filled boxes from Freeman and Hayes (1992); geoporphyrins used as a biomarker. Open box from Pagani et al. (1999a,b); $C_{37:2}$ alkenones used as a biomarker. Box labeled "s" from Stott (1992) (does not include estimates from P–E δ^{13}C excursion). Middle line represents the "best estimate" predictions of Berner and Kothavala (2001), while the two straddling lines represent error estimates based on sensitivity analyses. RCO_2 units of Berner and Kothavala (2001) converted to PCO_2 as in Fig. 13.

ranging taxa. Thus, the phytoplankton and stomatal proxies should be relied upon for Tertiary (and possibly Cretaceous) reconstructions, while the pedogenic carbonate proxy yields the most useful CO_2 estimates for the pre-Tertiary.

Despite the wide variety of assumptions made for each method, a surprisingly coherent picture is emerging of Phanerozoic PCO_2 change (see Figs. 13–16). The largest discrepancy exists between some of the Paleogene estimates of Pearson and Palmer

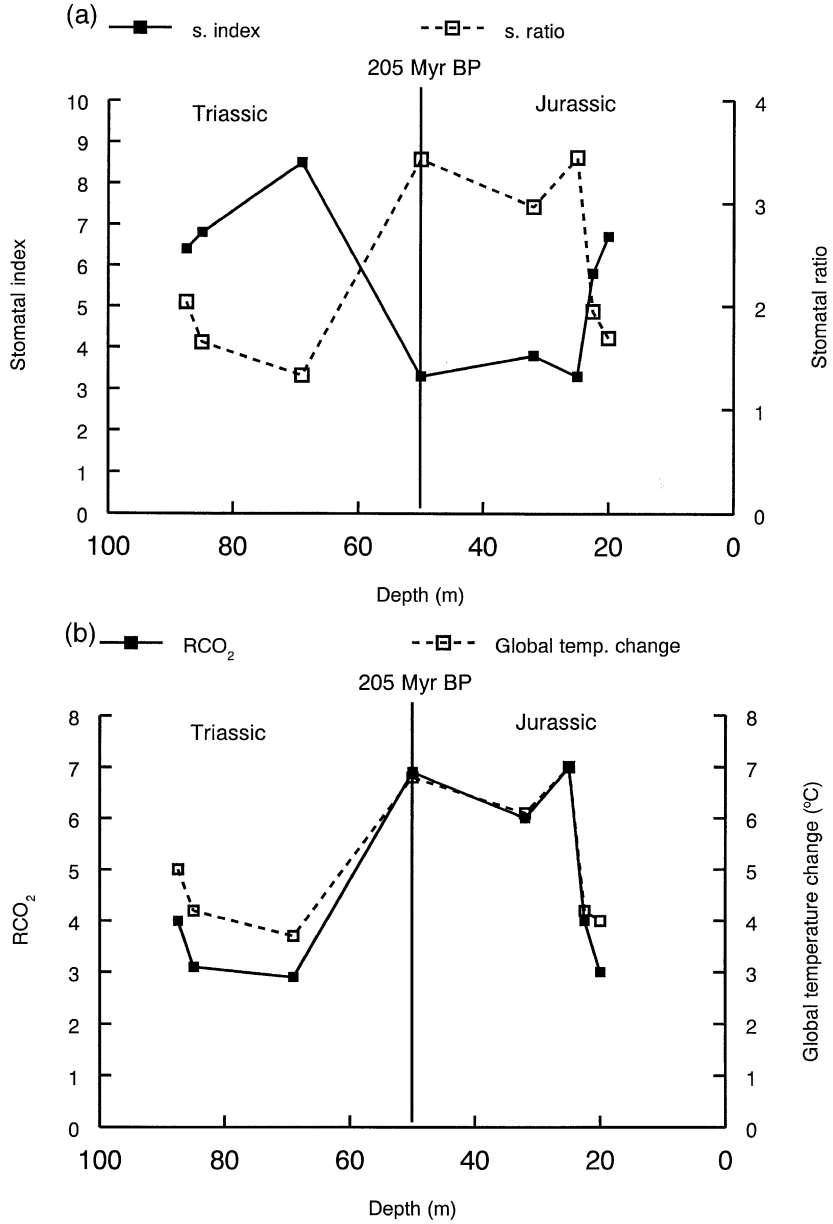

Fig. 17. Changes in the (a) stomatal index and stomatal ratio of fossil Ginkgo and cycad taxa from Greenland, (b) ratio of atmospheric CO_2 in the past relative to the pre-industrial value (RCO_2) and calculated change in global temperature, and (c) calculated changes in leaf width with and without the reconstructed changes in CO_2 and temperature and observed changes in leaf width across the Triassic–Jurassic boundary from the Greenland fossils (redrawn from McElwain et al., 1999).

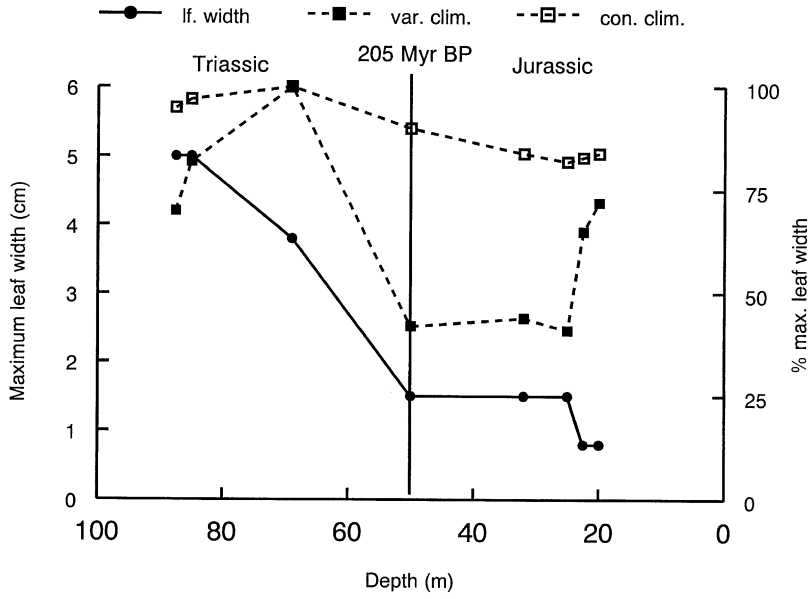

Fig. 17 (*continued*).

(2000) using the boron isotope method and the other methods (compare Fig. 15 with Figs. 13, 14 and 16). As discussed above (Section 6.2), however, these boron-derived estimates are probably not well constrained. Another discrepancy exists between the pedogenic carbonate estimates of Ekart et al. (1999) and the geochemical predictions of GEOCARB for the late Carboniferous and early Permian, i.e., the later stages of the Permo-Carboniferous glaciation (see Fig. 14). Ekart et al. (1999) used the marine carbonate $\delta^{13}C$ record of Veizer et al. (1999) to predict the $\delta^{13}C$ of the pedogenic carbonate's associated organic matter. This procedure decreases the precision of PCO_2 estimates (see Section 4.4). The PCO_2 discrepancy largely disappears if the δ_{occ} from Popp et al. (1986) are used instead of Veizer et al. (1999) (see Fig. 14). Alternatively, the discrepancy may be an artifact of the differing temporal resolutions of the two methods. Unlike the GEOCARB model, the pedogenic carbonate proxy has the potential to resolve short-lived (10^3–10^4 year) PCO_2 excursions. If true, this example highlights the importance of considering temporal resolution when comparing PCO_2 estimates from multiple methods.

Nevertheless, it is important to apply multiple PCO_2 proxies for a given time interval. We might envisage, for example, the complementary use of stomata and phytoplankton to detect CO_2 changes across the K–T boundary or the P–E boundary. Similarly, the stomatal proxy might usefully be applied across the Cenomanian–Turonian boundary where phytoplankton and terrestrial plant $\delta^{13}C$ shifts have indirectly identified a possible abrupt fall in CO_2 (Kuypers et al., 1999).

9. Independent testing of paleo-CO_2 estimates

An important feature of the all of the methods of paleo-CO_2 reconstructions reviewed here is the need to seek independent evidence for an associated change in climate. For the geochemical carbon cycle model predictions and paleosol estimates, times of low global CO_2 concentrations over the Phanerozoic generally coincide with episodes of major glaciations (Berner, 1998; Crowley, 2000), with the exception of the Ordovician when the solar constant was some 4–5% lower than now. Other indicators of global climate could also be deployed for this purpose (Parrish, 1998) but are only rarely used. Instead, the recourse typically taken has been to compare PCO_2

estimates between different methods (Berner, 1998; Ekart et al., 1999; Pearson and Palmer, 1999).

Perhaps because the stomatal paleo-CO_2 proxy approach is still in its infancy relative to most of the other CO_2 proxies, and regarded as somewhat controversial, where changes in CO_2 have been detected using this method more effort has been made to seek independent evidence of global change from the geologic record. For example, Neogene oscillations in atmospheric CO_2 inferred from changes in the SI of fossil oak leaves were found to correlate with climatic records determined from fossil pollen records in the Lower Rhynie Embayment (van der Burgh et al., 1993). Low SI values, i.e., high CO_2 episodes, correlated with warm climatic periods indicated from the fossil pollen assemblages. Reaching back further into the geologic record, Cleal et al. (1999) tracked a decrease in the SD and SI of pteridiosperm *Neuropteris ovata* fronds through the Westphalian and into the Cantabrian of the Upper Carboniferous with the inference atmospheric CO_2 partial pressure rose through this time. These authors then found secure evidence that the postulated CO_2 increase correlated with a decrease in the extent of glacial deposits in Gondwana and the reduced burial of terrestrial organic matter resulting from the loss of tropical wetland forests. This example therefore provides a case where changes in fossil plant morphology yield a global signal of CO_2 change of considerable antiquity.

Recent work has shown that it is possible to utilize the relatively rapid response time of the stomatal CO_2 method to detect abrupt CO_2 changes, in particular across the Triassic–Jurassic (T–J) boundary (205.7 Ma) (McElwain et al., 1999). The T–J boundary is of interest because an absence of secure marine geochemical records of climate change at this time means that the causes of this, the third largest extinction in the Phanerozoic, continue to remain uncertain. In this context, it is interesting to note that the timing of all of the major animal extinction events over the past 500 m.y. differs from that of plant extinction events. Therefore, fossil plants are potentially able to provide enlightening records of environmental change during major faunal mass extinction events.

McElwain et al. (1999) reported that the SI of fossil Gingko and Cycad taxa showed marked reductions across the T–J boundary that were mirrored when stomatal ratios were calculated from SI measurements on their nearest living equivalents (Fig. 17a). Conversion of the SR values to PCO_2 values indicated that the atmospheric CO_2 concentration increased massively from $\sim$700 to $\sim$1600 ppmV across the boundary with associated global 'greenhouse' warming (Fig. 17b). This CO_2 increase coincided with independent evidence for extensive volcanic activity during the breakup of Pangea (Marzoli et al., 1999), and moreover, the quantity of CO_2 required to increase the atmospheric concentration by this amount is well within that estimated to be have been released during the production of flood basalts of the Central Atlantic Magmatic Province (CAMP). The timing of the CAMP formation and its temporal brevity, determined from $^{40}Ar/^{39}Ar$ dating, support its possible involvement in the T–J boundary extinction (Marzoli et al., 1999; McElwain et al., 1999).

The fossil plants themselves also provide evidence for global climatic warming across the T–J boundary (McElwain et al., 1999). Analysis of changes in the morphologies of fossil leaves down through the different plant beds in Greenland show that the major floral turnover indicated by pollen analysis was linked to the extinction of broad-leaved taxa and the survival of those groups possessing finely divided or dissected leaf morphologies (Fig. 17c). Energy budget calculations for individual leaves, based on several key physiological attributes, indicate that wide leaves with limited convective cooling capacity, because of a low boundary layer conductance, would have quickly reached lethal temperatures for plants distributed at low paleolaltitudes, if the CO_2 increase and global warming had actually occurred (Fig. 17c). In contrast, if the CO_2 and global temperatures increases implied by the stomatal data were simply artifacts of the datasets, and both had remained constant, then no selective pressures would have operated for any observed reduction in leaf width to maintain their temperature below lethal thresholds (Fig. 17c). This integration of stomatal-based paleo-CO_2 estimates with independent data sources reinforces the view that global atmospheric signals can be derived from plant fossils and strengthens our confidence in the approach. As new approaches for interpreting changes in different

components of the global carbon cycle emerge (e.g., Haug et al., 1999) then it should be possible to devise alternative means of testing proxy estimates of PCO_2 change against independent geologic data sources.

Acknowledgements

DLR and RAB were partially supported by DOE grant DE-FGO_2-95ER14522. DLR also acknowledges support from a NSF Graduate Research Fellowship. DJB gratefully acknowledges funding through a Royal Society University Research Fellowship and the Natural Environment Research Council, UK (award no. GR3/11900). We thank S. Wofsy, B. Munger, M. Goulden, and C. Barford for providing canopy CO_2 data from Harvard Forest. We also thank L. Kump and W. Chaloner for constructive comments.

References

Andrews, J.E., Tandon, S.K., Dennis, P.F., 1995. Concentration of carbon dioxide in the Late Cretaceous atmosphere. Journal of the Geological Society (London) 152, 1–3.

Andrusevich, V.E., Engel, M.H., Zumberge, J.E., 2000. Effects of paleolatitude on the stable carbon isotope composition of crude oils. Geology 28, 847–850.

Arens, N.C., Jahren, A.H., Amundson, R., 2000. Can C_3 plants faithfully record the carbon isotopic composition of atmospheric carbon dioxide? Paleobiology 26, 137–164.

Arthur, M.A., Dean, W.E., Claypool, G.E., 1985. Anomalous ^{13}C enrichment in modern marine organic carbon. Nature 315, 216–218.

Baker, P.A., Gieskes, J.M., Elderfield, H., 1982. Diagenesis of carbonates in deep-sea sediments—evidence from Sr/Ca ratios and interstitial dissolved Sr^{2+} data. Journal of Sedimentary Petrology 52, 71–82.

Baver, L.D., Gardner, W.H., Gardner, W.R., 1972. Soil Physics. Wiley, New York.

Bazzaz, F.A., Williams, W.E., 1991. Atmospheric CO_2 concentrations within a mixed forest: implications for seedling growth. Ecology 72, 12–16.

Beerling, D.J., 1993. Changes in the stomatal density of *Betula nana* leaves in response to increases in atmospheric carbon dioxide concentration since the late-glacial. Special Papers in Palaeontology 49, 181–187.

Beerling, D.J., 1996. ^{13}C discrimination by fossil leaves during the late-glacial climate oscillation 12–10 ka BP: measurements and physiological controls. Oecologia 108, 29–37.

Beerling, D.J., 1998a. Atmospheric carbon dioxide, past climates and the plant fossil record. Botanical Journal of Scotland 51, 49–68.

Beerling, D.J., 1998b. The future as the key to the past. Trends in Ecology and Evolution 13, 311–316.

Beerling, D.J., 1999. Stomatal density and index: theory and application. In: Jones, T.P., Rowe, N.P. (Eds.), Fossil Plants and Spores: Modern Techniques. Geological Society, London, pp. 251–256.

Beerling, D.J., 2000. Global terrestrial productivity in the Mesozoic. In: Hart, M.B. (Ed.), Past, Present and Future Climates. Geological Society of London Special Publication 181, pp. 17–32.

Beerling, D.J., Chaloner, W.G., 1992. Stomatal density as an indicator of atmospheric CO_2 concentration. Holocene 2, 71–78.

Beerling, D.J., Chaloner, W.G., 1993. Evolutionary responses of stomatal density to global CO_2 change. Biological Journal of the Linnean Society 48, 343–353.

Beerling, D.J., Kelly, C.K., 1997. Stomatal density responses of temperate woodland plants over the past seven decades of CO_2 increase: a comparison of Salisbury (1927) with contemporary data. American Journal of Botany 84, 1572–1583.

Beerling, D.J., Woodward, F.I., 1996a. Stomatal density responses to global change. Advances in Bioclimatology 4, 171–221.

Beerling, D.J., Woodward, F.I., 1996b. Palaeo-ecophysiological perspectives on plant responses to global change. Trends in Ecology and Evolution 11, 20–23.

Beerling, D.J., Woodward, F.I., 1997. Changes in land plant function over the Phanerozoic: reconstructions based on the fossil record. Botanical Journal of the Linnean Society 124, 137–153.

Beerling, D.J., Chaloner, W.G., Huntley, B., Pearson, J.A., Tooley, M.J., 1993. Stomatal density responds to the glacial cycle of environmental change. Proceedings of the Royal Society of London, Series B 251, 133–138.

Beerling, D.J., Birks, H.H., Woodward, F.I., 1995. Rapid late-glacial atmospheric CO_2 changes reconstructed from the stomatal density record of fossil leaves. Journal of Quaternary Science 10, 379–384.

Berner, R.A., 1991. A model for atmospheric CO_2 over Phanerozoic time. American Journal of Science 291, 339–376.

Berner, R.A., 1994. GEOCARB II: a revised model of atmospheric CO_2 over Phanerozoic time. American Journal of Science 294, 56–91.

Berner, R.A., 1998. The carbon cycle and CO_2 over Phanerozoic time: the role of land plants. Philosophical Transactions of the Royal Society of London, Series B 353, 75–82.

Berner, R.A., 1999. A new look at the long-term carbon cycle. GSA Today 9 (11), 1–6.

Berner, R.A., Caldeira, K., 1997. The need for mass balance and feedback in the geochemical carbon cycle. Geology 25, 955–956.

Berner, R.A., Canfield, D., 1989. A new model for atmospheric oxygen over Phanerozoic time. American Journal of Science 289, 333–361.

Berner, R.A., Kothavala, Z., 2001. GEOCARB III: a revised

model of atmospheric CO_2 over Phanerozoic time. American Journal of Science (in review).

Berner, R.A., Lasaga, A.C., Garrels, R.M., 1983. The carbonate–silicate geochemical cycle and its effect on atmospheric carbon dioxide over the past 100 millions years. American Journal of Science 283, 641–683.

Berner, R.A., Petsch, S.T., Lake, J.A., Beerling, D.J., Popp, B.N., Lane, R.S., Laws, E.A., Westley, M.B., Cassar, N., Woodward, F.I., Quick, W.P., 2000. Isotope fractionation and atmospheric oxygen: implications for Phanerozoic O_2 evolution. Science 287, 1630–1633.

Bettarini, I., Miglietta, F., Raschi, A., 1997. Studying morpho-physiological responses of *Scirpus lacustris* from naturally CO_2-enriched environments. In: Rachi, A., Miglietta, F., Tognetti, R., van Gardingen, P.R. (Eds.), Plant Responses to Elevated CO_2. Cambridge Univ. Press, Cambridge, pp. 134–147.

Bettarini, I., Vaccari, F.P., Miglietta, F., 1998. Elevated CO_2 concentrations and stomatal density: observations from 17 plant species growing in a CO_2 spring in central Italy. Global Change Biology 4, 17–22.

Bidigare, R.R., Fluegge, A., Freeman, K.H., Hanson, K.L., Hayes, J.M., Hollander, D., Jasper, J.P., King, L.L., Laws, E.A., Milder, J., Millero, F.J., Pancost, R., Popp, B.N., Steinberg, P.A., Wakeham, S.G., 1997. Consistent fractionation of ^{13}C in nature and in the laboratory: growth-rate effects in some haptophyte algae. Global Biogeochemical Cycles 11, 279–292.

Bidigare, R.R., Fluegge, A., Freeman, K.H., Hanson, K.L., Hayes, J.M., Hollander, D., Jasper, J.P., King, L.L., Laws, E.A., Milder, J., Millero, F.J., Pancost, R., Popp, B.N., Steinberg, P.A., Wakeham, S.G., 1999a. Correction to "Consistent fractionation of ^{13}C in nature and in the laboratory: growth-rate effects in some haptophyte algae" by R.R. Bidigare et al. Global Biogeochemical Cycles 13, 251–252.

Bidigare, R.R., Hanson, K.L., Buesseler, K.O., Wakeham, S.G., Freeman, K.H., Pancost, R.D., Millero, F.J., Steinberg, P., Popp, B.N., Latasa, M., Landry, M.R., Laws, E.A., 1999b. Iron-stimulated changes in ^{13}C fractionation and export by equatorial Pacific phytoplankton: toward a paleogrowth rate proxy. Paleoceanography 14, 589–595.

Birks, H.H., Eide, W., Birks, H.J.B., 1999. Early Holocene atmospheric CO_2 concentrations. Science 286, 1815a.

Bocherens, H., Friis, E.M., Mariotti, A., Pedersen, K.R., 1993. Carbon isotopic abundances in Mesozoic and Cenozoic fossil plants: palaeoecological implications. Lethaia 26, 347–358.

Bounoua, L., Collatz, G.J., Sellers, P.J., Randall, D.A., Dazlich, D.A., Los, S.O., Berry, J.A., Fung, I., Tucker, C.J., Field, C.B., Jensen, T.G., 1999. Interactions between vegetation and climate: radiative and physiological effects of a doubled atmospheric CO_2. Journal of Climate 12, 309–324.

Brassell, S.C., Eglinton, G., Marlowe, I.T., Pfaumann, U., Sarnthein, M., 1986. Molecular stratigraphy: a new tool for climatic assessment. Nature 320, 129–133.

Brook, G.A., Folkoff, M.E., Box, E.O., 1983. A world model of soil carbon dioxide. Earth Surface Landforms 8, 79–88.

Buchmann, N., Kao, W.Y., Ehleringer, J.R., 1996. Carbon dioxide concentrations within forest canopies: variations with time, stand structure and vegetation type. Global Change Biology 2, 421–433.

Budyko, M.I., Ronov, A.B., Yanshin, A.L., 1987. History of the Earth's Atmosphere. Springer, Berlin.

Burns, B.D., Beardall, J., 1987. Utilization of inorganic carbon by marine microalgae. Journal of Experimental Marine Biology and Ecology 107, 75–86.

Caldeira, K., 1992. Enhanced Cenozoic chemical weathering and the subduction of pelagic carbonate. Nature 357, 578–581.

Caldeira, K., Kasting, J.F., 1992. The life-span of the biosphere revisited. Nature 360, 721–723.

Cerling, T.E., 1984. The stable isotopic composition of modern soil carbonate and its relationship to climate. Earth and Planetary Science Letters 71, 229–240.

Cerling, T.E., 1991. Carbon dioxide in the atmosphere: evidence from Cenozoic and Mesozoic paleosols. American Journal of Science 291, 377–400.

Cerling, T.E., 1992a. Further comments on using carbon isotopes in palaeosols to estimate the CO_2 content of the paleo-atmosphere. Journal of the Geological Society (London) 149, 673–675.

Cerling, T.E., 1992b. Use of carbon isotopes in paleosols as an indicator of the $P(CO_2)$ of the paleoatmosphere. Global Biogeochemical Cycles 6, 307–314.

Cerling, T.E., 1999. Stable carbon isotopes in palaeosol carbonates. Special Publications of the International Association of Sedimentologists 27, 43–60.

Cerling, T.E., Quade, J., Wang, Y., Bowman, J.R., 1989. Carbon isotopes in soils and palaeosols as ecology and palaeoecology indicators. Nature 341, 138–139.

Cerling, T.E., Quade, J., Ambrose, S.D., Sikes, N.E., 1991a. Fossil soils, grasses, and carbon isotopes from Fort Ternan, Kenya: grassland or woodland? Journal of Human Evolution 21, 295–306.

Cerling, T.E., Solomon, D.K., Quade, J., Bowman, J.R., 1991b. On the isotopic composition of carbon in soil carbon dioxide. Geochimica et Cosmochimica Acta 55, 3403–3405.

Ciais, P., 1999. Restless carbon pools. Nature 398, 111–112.

Clark, D.B., Clark, D.A., Grayum, M.H., 1992. Leaf demography of a neotropical rain forest cycad, *Zamia skinneri* (Zamiaceae). American Journal of Botany 79, 28–33.

Cleal, C.J., James, R.M., Zodrow, E.L., 1999. Variation in stomatal density in the Late Carboniferous gymnosperm frond *Neuropteris ovata*. Palaios 14, 180–185.

Clifford, S.C., Black, C.R., Roberts, J.A., Stronach, I.M., Singleton-Jones, P.R., Mohamed, A.D., Azam-Ali, S.N., 1995. The effect of elevated atmospheric CO_2 and drought on stomatal frequency in groundnut (*Arachis hypogaea* (L.)). Journal of Experimental Botany 46, 847–852.

Conte, M.H., Volman, J.K., Eglinton, G., 1994. Lipid biomarkers of the Haptophyta. In: Green, J.C., Leadbeater, B.S.C. (Eds.), The Haptophyte Algae. Clarendon Press, Oxford, pp. 351–377.

Cowan, I.R., 1977. Stomatal behaviour and environment. Advances in Botanical Research 77, 1176–1227.

Craig, H., 1953. The geochemistry of stable carbon isotopes. Geochimica et Cosmochimica Acta 3, 53–92.

Crowley, T.J., 2000. Carbon dioxide and Phanerozoic climate. In:

Huber, B.T., MacLeod, K.G., Wing, S.L. (Eds.), Warm Climates in Earth History. Cambridge Univ. Press, Cambridge, pp. 425–444.

Davidson, G.R., 1995. The stable isotopic composition and measurement of carbon in soil CO2. Geochimica et Cosmochimica Acta 59, 2485–2489.

Dean, W.E., Arthur, M.A., Claypool, G.E., 1986. Depletion of ^{13}C in Cretaceous marine organic matter: source, diagenetic, or environmental signal? Marine Geology 70, 119–157.

Degens, E.T., Guillard, R.R.L., Sackett, W.M., Hellebust, J.A., 1968. Metabolic fractionation of carbon isotopes in marine plankton: I. Temperature and respiration experiments. Deep-Sea Research 15, 1–9.

Deines, P., 1980. The isotopic composition of reduced organic carbon. In: Fritz, P., Fontes, J.Ch. (Eds.), Handbook of Environmental Geochemistry, vol. 1. Elsevier, Amsterdam, pp. 329–406.

De La Rocha, C.L., De Paolo, D.J., 2000. Isotopic evidence for variations in the marine calcium cycle over the Cenozoic. Science 289, 1176–1178.

Derry, L.A., France-Lanord, C., 1996. Neogene growth of the sedimentary organic carbon reservoir. Paleoceanography 11, 267–275.

Dörr, H., Münnich, K.O., 1990. ^{222}Rn flux and soil air concentration profiles in West Germany. Soil ^{222}Rn as tracer for gas transport in the unsaturated soil zone. Tellus 42B, 20–28.

Driese, S.G., Mora, C.I., Cotter, E., Foreman, J.L., 1992. Paleopedology and stable isotope chemistry of Late Silurian vertic paleosols, Bloomsburg Formation, central Pennsylvania. Journal of Sedimentary Petrology 62, 825–841.

Edwards, D.E., 1998. Climate signals in Palaeozoic land plants. Philosophical Transactions of the Royal Society of London, Series B 353, 141–157.

Ehleringer, J.R., Cerling, T.E., 1995. Atmospheric CO_2 and the ratio of intercellular to ambient CO_2 concentrations in plants. Tree Physiology 15, 105–111.

Ekart, D.D., Cerling, T.E., Moñtanez, I.P., Tabor, N.J., 1999. A 400 million year carbon isotope record of pedogenic carbonate: implications for paleoatmospheric carbon dioxide. American Journal of Science 299, 805–827.

Ekstrom, A., Fookes, C.J.R., Hambley, T., Loehh, J., Miller, S.A., Taylor, J.C., 1983. Determination of the crystal structure of a petroporphyrin isolated from oil shale. Nature 306, 173–174.

Elick, J.M., Mora, C.I., Driese, S.G., 1999. Elevated atmospheric CO_2 levels and expansion of early vascular land plants: stable isotope evidence from the Battery Point Fm. (Early to Middle Devonian), Gaspé Bay, Canada. GSA Abstracts with Programs 31, A-159.

Estiarte, M., Peñuelas, J., Kimball, B.A., Idso, S.B., LaMorte, R.L., Pinter, P.J., Wall, G.W., Garcia, R.L., 1994. Elevated CO_2 effects on stomatal density of wheat and sour orange trees. Journal of Experimental Botany 45, 1665–1668.

Evans, J.R., Sharkey, T.D., Berry, J.A., Farquhar, G.D., 1986. Carbon isotope discrimination measured concurrently with gas exchange to investigate CO_2 diffusion in leaves of higher plants. Australian Journal of Plant Physiology 13, 281–292.

Farquhar, G.D., Richards, R.A., 1984. Isotopic composition of plant carbon correlates with water-use efficiency of wheat genotypes. Australian Journal of Plant Physiology 11, 539–552.

Farquhar, G.D., O'Leary, M.H., Berry, J.A., 1982. On the relationship between carbon isotope discrimination and the intercellular carbon dioxide concentration in leaves. Australian Journal of Plant Physiology 9, 121–137.

Farrimond, P., Eglinton, G., Brassell, S.C., 1986. Alkenones in Cretaceous black shales, Blake-Bahama Basin, western North Atlantic. Organic Geochemistry 10, 897–903.

Fernández, M.D., Pieter, A., Donso, C., Tezara, W., Azkue, M., Herrera, C., Rengifo, E., Herrera, A., 1998. Effects of a natural source of very high CO_2 concentration on the leaf gas exchange, xylem water potential and stomatal characteristics of *Spatiphylum cannifolium* and *Bauhinia multivervia*. New Phytologist 138, 689–697.

France-Lanord, C., Derry, L.A., 1997. Organic carbon burial forcing of the carbon cycle from Himalayan erosion. Nature 390, 65–67.

François, L.M., Godderis, Y., 1998. Isotopic constraints on the Cenozoic evolution of the carbon cycle. Chemical Geology 145, 177–212.

François, L.M., Walker, J.C.G., 1992. Modeling the Phanerozoic carbon cycle and climate constraints from the $^{87}Sr/^{86}Sr$ isotopic ratio of seawater. American Journal of Science 292, 81–135.

François, R., Altabet, M.A., Goericke, R., McCorkle, D.C., Brunet, C., Poisson, A., 1993. Changes in the $\delta^{13}C$ of surface water particulate organic matter across the subtropical convergence in the S.W. Indian Ocean. Global Biogeochemical Cycles 7, 627–644.

Freeman, K.H., Hayes, J.M., 1992. Fractionation of carbon isotopes by phytoplankton and estimates of ancient CO_2 levels. Global Biogeochemical Cycles 6, 185–198.

Friedli, H., Lötscher, H., Oeschger, H., Siegenthaler, U., Stauffer, B., 1986. Ice core record of the $^{13}C/^{12}C$ ratio of atmospheric CO_2 in the past two centuries. Nature 324, 237–238.

Fry, B., Wainwright, S.C., 1991. Diatom sources of ^{13}C-rich carbon in marine food webs. Marine Ecology: Progress Series 76, 149–157.

Gale, J., 1972. Availability of carbon dioxide for photosynthesis at high altitudes: theoretical considerations. Ecology 53, 494–497.

Ghosh, P., Bhattacharya, S.K., Jani, R.A., 1995. Palaeoclimate and palaeovegetation in central India during the Upper Cretaceous based on stable isotope composition of the palaeosol carbonates. Palaeogeography, Palaeoclimatology, Palaeoecology 114, 285–296.

Gibbs, M.T., Barron, E.J., Kump, L.R., 1997. An atmospheric pCO_2 threshold for glaciation in the Late Ordovician. Geology 25, 447–450.

Gibbs, M.T., Bluth, G.J.S., Fawcett, P.J., Kump, L.R., 1999. Global chemical erosion over the last 250 my: variations due to changes in paleogeography, paleoclimate, and paleogeology. American Journal of Science 299, 611–651.

Gile, L.H., Peterson, F.F., Grossman, R.B., 1979. The Desert Project Soil Monograph. U.S. Soil Conservation Service, Washington.

Givnish, T.J., 1988. Adaptation to sun and shade: a whole plant perspective. Australian Journal of Plant Physiology 15, 63–92.

Godderis, Y., François, L.M., 1995. The Cenozoic evolution of the strontium and carbon cycles: relative importance of continental erosion and mantle exchanges. Chemical Geology 126, 169–190.

Godderis, Y., François, L.M., 1996. Balancing the Cenozoic carbon and alkalinity cycles: constraints from isotopic records. Geophysical Research Letters 23, 3743–3746.

Goericke, R., Montoya, J.P., Fry, B., 1994. Physiology of isotope fractionation in algae and cyanobacteria. In: Lajtha, K., Michener, R.H. (Eds.), Stable Isotopes in Ecology. Blackwell Science, Oxford, pp. 187–221.

Grace, J., Lloyd, J., McIntyre, J., Miranda, A., Meir, P., Miranda, H., Moncrieff, J., Massheder, J., Wright, I., Gash, J., 1995. Fluxes of carbon dioxide and water vapour over an undisturbed tropical forest in south-west Amazonia. Global Change Biology 1, 1–13.

Haug, G.H., Sigman, D.M., Tiedemann, R., Pedersen, T.F., Sarnthein, M., 1999. Onset of permanent stratification in the subarctic Pacific Ocean. Nature 401, 779–782.

Hayes, J.M., 1993. Factors controlling ^{13}C contents of sedimentary organic compounds: principles and evidence. Marine Geology 113, 111–125.

Hayes, J.M., Takigiku, R., Ocampo, R., Callot, H.J., Albrecht, P., 1987. Isotopic compositions and probable origins of organic molecules in the Eocene Messel shale. Nature 329, 48–51.

Hayes, J.M., Freeman, K.H., Popp, B.N., Hoham, C.H., 1989a. Compound-specific isotopic analyses: a novel tool for reconstruction of ancient biogeochemical processes. Organic Geochemistry 16, 1115–1128.

Hayes, J.M., Popp, B.N., Takigiku, R., Johnson, M.W., 1989b. An isotopic study of biogeochemical relationships between carbonates and organic carbon in the Greenhorn Formation. Geochimica et Cosmochimica Acta 53, 2961–2972.

Hayes, J.M., Strauss, H., Kaufman, A.J., 1999. The abundance of ^{13}C in marine organic matter and isotopic fractionation in the global biogeochemical cycle of carbon during the past 800 Ma. Chemical Geology 161, 103–125.

Hemming, N.G., Hanson, G.N., 1992. Boron isotopic composition and concentration in modern marine carbonates. Geochemica et Cosmochimica Acta 56, 537–543.

Hinga, K.R., Arthur, M.A., Pilson, M.E.Q., Whitaker, D., 1994. Carbon isotope fractionation by marine phytoplankton in culture: the effects of CO_2 concentration, pH, temperature, and species. Global Biogeochemical Cycles 8, 91–102.

Hollander, D.J., McKenzie, J.A., 1991. CO_2 control on carbon-isotope fractionation during aqueous photosynthesis: a paleo-pCO_2 barometer. Geology 19, 929–932.

Hovenden, M.J., Schimanski, L.J., 2000. Genotypic differences in growth and stomatal morphology of southern beech, *Nothofagus cunninghamii*, exposed to depleted CO_2 concentrations. Australian Journal of Plant Physiology 27, 281–287.

Indermühle, A., Stauffer, B., Stocker, T.F., Raynaud, D., Barnola, J.M., 1999a. Early Holocene atmospheric CO_2 concentrations. Science 286, 1815a.

Indermühle, A., Stocker, T.F., Joos, F., Fischer, H., Smith, H.J., Wahlen, M., Deck, B., Mastroianni, D., Tschumi, J., Blunier, T., Meyer, R., Stauffer, B., 1999b. Holocene carbon-cycle dynamics based on CO_2 trapped in ice at Taylor Dome, Antarctica. Nature 398, 121–126.

Jarvis, P.G., McNaughton, K.G., 1985. Stomatal control of transpiration: scaling up from leaf to region. Advances in Ecological Research 15, 1–49.

Jasper, J.P., Hayes, J.M., 1990. A carbon isotope record of CO_2 levels during the late Quaternary. Nature 347, 462–464.

Jasper, J.P., Hayes, J.M., Mix, A.C., Prahl, F.G., 1994. Photosynthetic fractionation of ^{13}C and concentrations of dissolved CO_2 in the central equatorial Pacific during the last 255,000 years. Paleoceanography 9, 781–798.

Jones, H.G., 1992. Plants and Microclimate. Cambridge Univ. Press, Cambridge.

Jones, T.P., 1994. ^{13}C enriched Lower Carboniferous fossil plants from Donegal, Ireland: carbon isotope constraints on taphonomy, diagenesis and palaeoenvironment. Review of Palaeobotany and Palynology 81, 53–64.

Jones, T.P., Rowe, N.P. (Eds.) 1999. Fossil Plants and Spores: Modern Techniques. Geological Society, London.

Kelly, C.K., Beerling, D.J., 1995. Plant life form, stomatal density and taxonomic relatedness: a reanalysis of Salisbury (1927). Functional Ecology 9, 422–431.

Kennett, J.P., 1982. Marine Geology. Prentice-Hall, Englewood Cliffs.

Kirkham, D., Powers, W.L., 1972. Advanced Soil Physics. Wiley-Interscience, New York.

Koch, P.L., Zachos, J.C., Gingerich, P.D., 1992. Correlation between isotope records in marine and continental carbon reservoirs near the Palaeocene/Eocene boundary. Nature 358, 319–322.

Körner, Ch., Bannister, P., Mark, A.F., 1986. Altitudinal variation in stomatal conductance, nitrogen content and leaf anatomy in different plant life forms in New Zealand. Oecologia 69, 577–588.

Kothavala, Z., Oglesby, R.J., Saltzman, B., 1999. Sensitivity of equilibrium surface temperature of CCM3 to systematic changes in atmospheric CO_2. Geophysical Research Letters 26, 209–212.

Kump, L.R., Arthur, M.A., 1997. Global chemical erosion during the Cenozoic: weatherability balances the budgets. In: Ruddiman, W.F. (Ed.), Tectonic Uplift and Climate Change. Plenum, New York, pp. 399–426.

Kump, L.R., Arthur, M.A., 1999. Interpreting carbon-isotope excursions: carbonates and organic matter. Chemical Geology 161, 181–198.

Kump, L.R., Arthur, M.A., Patzkowsky, M.E., Gibbs, M.T., Pinkus, D.S., Sheenan, P.M., 1999. A weathering hypothesis for glaciation at high atmospheric pCO_2 during the Late Ordovician. Palaeoclimatology, Palaeogeography, Palaeoecology 152, 173–187.

Kundu, S.K., Tigerstedt, P.M.A., 1999. Variations in net photosynthesis, stomatal characteristics, leaf area and whole-plant phytomass production among ten provenances of neem (*Azadirachata indica*). Tree Physiology 19, 47–52.

Kürschner, W.M., 1997. The anatomical diversity of recent and fossil leaves of the durmast oak (*Quercus petraea* Lieblein / *Q. pseudocastanea* Goeppert)—implications for their use as biosensors of palaeoatmospheric CO_2 levels. Review of Palaeobotany and Palynology 96, 1–30.

Kürschner, W.M., van der Burgh, J., Visscher, H., Dilcher, D.L., 1996. Oak leaves as biosensors of late Neogene and early Pleistocene paleoatmospheric CO_2 concentrations. Marine Micropaleontology 27, 299–312.

Kürschner, W.M., Wagner, F., Visscher, E.H., Visscher, H., 1997. Predicting the response of leaf stomatal frequency to a future CO_2-enriched atmosphere: constraints from historical observations. Geologische Rundschau 86, 512–517.

Kuypers, M.M.M., Pancost, R.D., Sinninghe Damste, J.S.S., 1999. A large and abrupt fall in atmospheric CO_2 concentration during Cretaceous times. Nature 399, 342–345.

Lasaga, A.C., Berner, R.A., Garrels, R.M., 1985. An improved geochemical model of atmospheric CO_2 fluctuations over the past 100 million years. In: Sunquist, E.T., Broecker, W.S. (Eds.), The Carbon Cycle and Atmospheric CO_2: Natural Variations Archean to Present. Geophysical Monographs vol. 32. American Geophysical Union, 397.

Laws, E.A., Popp, B.N., Bidigare, R.R., Kennicutt, M.C., Macko, S.A., 1995. Dependence of phytoplankton carbon isotopic composition on growth rate and $[CO_2]_{aq}$: theoretical considerations and experimental results. Geochimica et Cosmochimica Acta 59, 1131–1138.

Laws, E.A., Bidigare, R.R., Popp, B.N., 1997. Effect of growth rate and CO_2 concentration on carbon isotopic fractionation by the marine diatom *Phaeodactylum tricornutum*. Limnology and Oceanography 42, 1552–1560.

Lee, Y.I., 1999. Stable isotopic composition of calcic paleosols of the Early Cretaceous Hasandong Formation, southeastern Korea. Palaeogeography, Palaeoclimatology, Palaeoecology 150, 123–133.

Lee, Y.I., Hisada, K., 1999. Stable isotopic composition of pedogenic carbonates of the Early Cretaceous Shimonoseki Subgroup, western Honshu, Japan. Palaeogeography, Palaeoclimatology, Palaeoecology 153, 127–138.

Lemarchand, D., Gaillardet, J., Lewin, É., Allègre, C.J., 2000. Boron isotope systematics in large rivers: implications for oceanic $\delta^{11}B$ secular variations. Nature (in review).

Liu, Y.-G., Schmitt, R.A., 1996. Cretaceous Tertiary phenomena in the context of seafloor rearrangements and $P(CO_2)$ fluctuations over the past 100 m.y. Geochimica et Cosmochimica Acta 60, 973–994.

Marlowe, I.T., Brassell, S.C., Eglinton, G., Green, J.C., 1990. Long-chain alkenones and alkyl alkenoates and the fossil coccolith record of marine sediments. Chemical Geology 88, 349–375.

Marzoli, A., Renne, P.R., Piccirillo, E.M., Ernesto, M., Belllieni, G., De Min, A., 1999. Extensive 200-million-year-old continental flood basalts of the central atlantic magmatice province. Science 284, 616–618.

Mason, E.A., Marrero, T.R., 1970. The diffusion of atoms and molecules. In: Bates, D.R., Esterman, I. (Eds.), Advances in Atomic and Molecular Physics, vol. 6. Academic Press, New York, pp. 155–226.

McCabe, B., 1985. The Dynamics of ^{13}C in Several New Zealand Lakes. PhD Thesis. University of Waikato, New Zealand.

McCauley, S.E., DePaolo, D.J., 1997. The marine $^{87}Sr/^{86}Sr$ and $\delta^{18}O$ records, Himalayan alkalinity fluxes and Cenozoic climate models. In: Ruddiman, W.F. (Ed.), Tectonic Uplift and Climate Change. Plenum, New York, pp. 427–467.

McElwain, J.C., 1998. Do fossil plants signal palaeoatmospheric CO_2 concentration in the geological past? Philosophical Transactions of the Royal Society of London, Series B 353, 83–96.

McElwain, J.C., Chaloner, W.G., 1995. Stomatal density and index of fossil plants track atmospheric carbon dioxide in the Palaeozoic. Annals of Botany 76, 389–395.

McElwain, J.C., Chaloner, W.G., 1996. The fossil cuticle as a skeletal record of environmental change. Palaios 11, 376–388.

McElwain, J., Mitchell, F.J.G., Jones, M.B., 1995. Relationship of stomatal density and index of *Salix cinerea* to atmospheric carbon dioxide concentrations in the Holocene. Holocene 5, 216–219.

McElwain, J.C., Beerling, D.J., Woodward, F.I., 1999. Fossil plants and global warming at the Triassic–Jurassic boundary. Science 285, 1386–1390.

Moffett, J.W., 1990. Microbially mediated cerium oxidation in sea water. Nature 345, 421–423.

Mook, W.G., Bommerson, J.C., Staberman, W.H., 1974. Carbon isotope fractionation between dissolved bicarbonate and gaseous carbon dioxide. Earth and Planetary Science Letters 22, 169–176.

Mora, C.I., Driese, S.G., 1999. Palaeoenvironment, palaeoclimate and stable carbon isotopes of Palaeozoic red-bed palaeosols, Appalachian Basin, USA and Canada. Special Publications of the International Association of Sedimentologists 27, 61–84.

Mora, C.I., Driese, S.G., Seager, P.G., 1991. Carbon dioxide in the Paleozoic atmosphere: evidence from carbon-isotope compositions of pedogenic carbonate. Geology 19, 1017–1020.

Mora, C.I., Driese, S.G., Colarusso, L.A., 1996. Middle and Late Paleozoic atmospheric CO_2 levels from soil carbonate and organic matter. Science 271, 1105–1107.

Morison, J.I.L., 1985. Sensitivity of stomata and water use efficiency to high CO_2. Plant, Cell and Environment 8, 467–474.

Muchez, P., Peeters, C., Keppens, E., Viaene, W.A., 1993. Stable isotopic composition of paleosols in the Lower Visan of eastern Belgium: evidence of evaporation and soil–gas CO_2. Chemical Geology 106, 389–396.

Nielsen, S.L., Gacia, E., Sand-Jensen, K., 1991. Land plants of amphibious *Littorella uniflora* (L.) Aschers. maintain utilization of CO_2 from the sediment. Oecologia 88, 258–262.

O'Leary, M.H., 1984. Measurement of the isotope fractionation associated with diffusion of carbon dioxide in aqueous solution. Journal of Physical Chemistry 88, 823–825.

Pagani, M., Arthur, M.A., Freeman, K.H., 1999a. Miocene evolution of atmospheric carbon dioxide. Paleoceanography 14, 273–292.

Pagani, M., Freeman, K.H., Arthur, M.A., 1999b. Late Miocene atmospheric CO_2 concentrations and the expansion of C_4 grasses. Science 285, 876–879.

Pagani, M., Freeman, K.H., Arthur, M.A., 2000. Isotope analyses of molecular and total organic carbon from Miocene sediments. Geochimica et Cosmochimica Acta 64, 37–49.

Palmer, M.R., Pearson, P.N., Cobb, S.J., 1998. Reconstructing past ocean pH-depth profiles. Science 282, 1468–1471.

Paoletti, E., Nourrisson, G., Garrec, J.P., Raschi, A., 1998. Modifications of the leaf surface structures of *Quercus ilex* L. in open, naturally CO_2-enriched environments. Plant, Cell and Environment 21, 1071–1075.

Parrish, J.T., 1998. Interpreting Pre-Quaternary Climate from the Geologic Record. Columbia Univ. Press, New York.

Pearson, P.N., Palmer, M.R., 1999. Middle Eocene seawater pH and atmospheric carbon dioxide concentrations. Science 284, 1824–1826.

Pearson, P.N., Palmer, M.R., 2000. Atmospheric carbon dioxide concentrations over the past 60 million years. Nature 406, 695–699.

Pedersen, O., Sand-Jensen, K., 1992. Adaptations of submerged *Lobelia dortmanna* to aerial life form: morphology, carbon sources and oxygen dynamics. Oikos 65, 89–96.

Petit, J.R., Jouzel, J., Raynaud, D., Barkov, N.I., Barnola, J.-M., Basile, I., Bender, M., Chappellaz, J., Davis, M., Delaygue, G., Delmotte, M., Kotlyakov, V.M., Legrand, M., Lipenkov, V.Y., Lorius, C., Pépin, L., Ritz, C., Saltzman, E., Stievenard, M., 1999. Climate and atmospheric history of the past 420,000 years from the Vostok ice core, Antarctica. Nature 399, 429–436.

Platt, N.H., 1989. Lacustrine carbonates and pedogenesis: sedimentology and origin of palustrine deposits from the Early Cretaceous Rupelo Formation, W. Cameros Basin, N. Spain. Sedimentology 36, 665–684.

Polley, H.W., Johnson, H.B., Marino, B.D., Mayeux, H.S., 1993. Increase in C_3 plant water-use efficiency and biomass over Glacial to present CO_2 concentrations. Nature 361, 61–64.

Poole, I., Weyers, J.D.B., Lawson, T., Raven, J.A., 1996. Variations in stomatal density and index: implications for palaeoclimate reconstructions. Plant, Cell and Environment 19, 705–712.

Popp, B.N., Anderson, T.F., Sandberg, P.A., 1986. Brachiopods as indicators of original isotopic compositions in some Paleozoic limestones. Bulletin of the Geological Society of America 97, 1262–1269.

Popp, B.N., Takigiku, R., Hayes, J.M., Louda, J.W., Baker, E.W., 1989. The post-Paleozoic chronology and mechanism of ^{13}C depletion in primary marine organic matter. American Journal of Science 289, 436–454.

Popp, B.N., Laws, E.A., Bidigare, R.R., Dore, J.E., Hanson, K.L., Wakeham, S.G., 1998. Effect of phytoplankton cell geometry on carbon isotopic fractionation. Geochimica et Cosmochimica Acta 62, 69–77.

Popp, B.N., Trull, T., Kenig, F., Wakeham, S.G., Rust, T.M., Tilbrook, B., Griffiths, F.B., Wright, S.W., Marchant, H.J., Bidigare, R.R., Laws, E.A., 1999. Controls on the carbon isotopic composition of Southern Ocean phytoplankton. Global Biogeochemical Cycles 13, 827–843.

Prahl, F.G., Wakeham, S.G., 1987. Calibration of unsaturation patterns in long-chain ketone compositions for palaeotemperature assessment. Nature 330, 367–369.

Quade, J., Cerling, T.E., Bowman, J.R., 1989. Systematic variations in the carbon and oxygen isotopic composition of pedogenic carbonate along elevation transects in the southern Great Basin, United States. Geological Society of America Bulletin 101, 464–475.

Rau, G.H., Takahashi, T., Des Mariais, D.J., 1989. Latitudinal variations in plankton $\delta^{13}C$: implications for CO_2 and productivity in past oceans. Nature 341, 516–518.

Rau, G.H., Froelich, P.N., Takahasi, T., Des Marais, D.J., 1991a. Does sedimentary organic $\delta^{13}C$ record variations in Quaternary ocean $[CO_{2(aq)}]$? Paleoceanography 6, 335–347.

Rau, G.H., Takahashi, T., Des Marais, D.J., Sullivan, C.W., 1991b. Particulate organic matter $\delta^{13}C$ variations across the Drake Passage. Journal of Geophysical Research 96, 15131–15135.

Rau, G.H., Takahasi, T., Des Marais, D.J., Repeta, D.J., Martin, J.H., 1992. The relationship between $\delta^{13}C$ of organic matter and $[CO_{2(aq)}]$ in ocean surface water: data from a JGOFS site in the northeast Atlantic Ocean and a model. Geochimica et Cosmochimica Acta 56, 1413–1419.

Raymo, M.E., 1997. Carbon cycle models—how strong are the constraints? In: Ruddiman, W.F. (Ed.), Tectonic Uplift and Climate Change. Plenum, New York, pp. 367–381.

Raymo, M.E., Ruddiman, W.F., 1992. Tectonic forcing of late Cenozoic climate. Nature 359, 117–122.

Reich, P.B., Uhl, C., Walters, M.B., Ellsworth, D.S., 1991. Leaf lifespan as a determinant of leaf structure and function among 23 amazonian tree species. Oecologia 86, 16–24.

Reinfelder, J.R., Kraepiel, A.M.L., Morel, F.M.M., 2000. Unicellular C_4 photosynthesis in a marine diatom. Nature 407, 996–999.

Retallack, G.J., 1988. Field recognition of paleosols. Geological Society of America Special Papers 216, 1–20.

Retallack, G.J., 1990. Soils of the Past. Unwin-Hyman, London.

Roeske, C.A., O'Leary, M.H., 1985. Carbon isotope effect on carboxylation of ribulose biphosphate catalyzed by ribulosebiphosphate carboxylase from *Rhodosprillum rubrum*. Biochemistry 24, 1603–1607.

Romanek, C.S., Grossman, E.L., Morse, J.W., 1992. Carbon isotopic fractionation in synthetic aragonite and calcite: effects of temperature and precipitation rate. Geochimica et Cosmochimica Acta 56, 419–430.

Royer, D.L., 1999. Depth to pedogenic carbonate horizon as a paleoprecipitation indicator? Geology 27, 1123–1126.

Royer, D.L., 2001. Stomatal density and stomatal index as indicators of atmospheric CO_2 concentration. Review of Palaeobotany and Palynology (in press).

Rundgren, M., Beerling, D., 1999. A Holocene CO_2 record from the stomatal index of sub-fossil *Salix herbacea* L. leaves from northern Sweden. Holocene 9, 509–513.

Salisbury, E.J., 1927. On the causes and ecological significance of stomatal frequency, with special reference to the woodland flora. Philosophical Transactions of the Royal Society of London, Series B 216, 1–65.

Sanyal, A., Hemming, N.G., Hanson, G.N., Broecker, W.S., 1995. Evidence for a higher pH in the glacial ocean from boron isotopes in foraminifera. Nature 373, 234–236.

Sanyal, A., Hemming, N.G., Broecker, W.S., Lea, D.W., Spero, H.J., Hanson, G.N., 1996. Oceanic *p*H control on the boron isotopic composition of foraminifera: evidence from culture experiments. Paleoceanography 11, 513–517.

Sharma, G.K., Dunn, D.B., 1968. Effect of environment on the cuticular features in *Kalanchoe fedschenkoi*. Bulletin of the Torrey Botanical Club 95, 464–473.

Sharma, G.K., Dunn, D.B., 1969. Environmental modifications of leaf surface traits in *Datura stramonium*. Canadian Journal of Botany 47, 1211–1216.

Sinha, A., Stott, L.D., 1994. New atmospheric pCO_2 estimates from paleosols during the late Paleocene/early Eocene global warming interval. Global and Planetary Change 9, 297–307.

Sloan, L.C., Rea, D.K., 1995. Atmospheric carbon dioxide and early Eocene climate: a general circulation modeling sensitivity study. Palaeogeography, Palaeoclimatology, Palaeoecology 119, 275–292.

Solomon, D.K., Cerling, T.E., 1987. The annual carbon dioxide cycle in a montane soil: observations, modeling, and implications for weathering. Water Resources Research 23, 2257–2265.

Spicer, R.A., 1981. The sorting and deposition of allochthonous plant material in a modern environment at Silwood Lake, Silwood Park, Berkshire, England. U.S. Geological Survey Professional Paper 1143, 1–77.

Spivack, A.J., You, C.-F., 1997. Boron isotopic geochemistry of carbonates and pore waters, Ocean Drilling Program Site 851. Earth and Planetary Science Letters 152, 113–122.

Spivack, A.J., You, C.-F., Smith, H.J., 1993. Foraminiferal boron isotope ratios as a proxy for surface ocean pH over the past 21 Myr. Nature 363, 149–151.

Stanhill, G., 1986. Water use efficiency. Advances in Agronomy 39, 53–85.

Stott, L.D., 1992. Higher temperatures and lower oceanic pCO_2: a climate enigma at the end of the Paleocene epoch. Paleoceanography 7, 395–404.

Suchecky, R.K., Hubert, J.F., Birney de Wit, C.C., 1988. Isotopic imprint of climate and hydrogeochemistry on terrestrial strata of the Triassic–Jurassic Hartford and Fundy Rift Basins. Journal of Sedimentary Petrology 58, 801–811.

Tajika, E., 1998. Climate change during the last 150 million years: reconstruction from a carbon cycle model. Earth and Planetary Science Letters 160, 695–707.

Tans, P.P., Fung, I.Y., Takahasi, T., 1990. Observational constraints on the global atmospheric CO_2 budget. Science 247, 1431–1438.

Tichá, I., 1982. Photosynthetic characteristics during ontogenesis of leaves. 7. Stomata density and sizes. Photosynthetica 16, 375–471.

Tognetti, R., Minnocci, A., Peñuelas, J., Raschi, A., Jones, M.B., 2000. Comparative field water relations of three Mediterranean shrub species co-occurring in a natural CO_2 vent. Journal of Experimental Botany 51, 1135–1146.

van de Water, P.K., Leavitt, S.W., Betancourt, J.L., 1994. Trends in stomatal density and $^{13}C/^{12}C$ ratios of *Pinus flexilis* needles during last glacial–interglacial cycle. Science 264, 239–243.

van der Burgh, J., Visscher, H., Dilcher, D.L., Kürschner, W.M., 1993. Paleoatmospheric signatures in Neogene fossil leaves. Science 260, 1788–1790.

Veizer, J., Ala, D., Azmy, K., Brucjschen, P., Buhl, D., Bruhn, F., Carden, G.A.F., Diener, A., Ebneth, S., Godderis, Y., Jasper, T., Korte, C., Pawellek, F., Podlaha, O.G., Strauss, H., 1999. $^{87}Sr/^{86}Sr$, $\delta^{13}C$ and $\delta^{18}O$ evolution of Phanerozoic seawater. Chemical Geology 161, 59–88.

Vengosh, A., Kolodny, Y., Starinsky, A., Chivas, A.R., McCulloch, M.T., 1991. Coprecipitation and isotopic fractionation of boron in modern biogenic carbonates. Geochimica et Cosmochimica Acta 55, 2901–2910.

Wagner, F., 1998. The influence of environment on the stomatal frequency in *Betula*. LPP Contributions Series 9, 1–102.

Wagner, F., Below, R., De Klerk, P., Dilcher, D.L., Joosten, H., Kürschner, W.M., Visscher, H., 1996. A natural experiment on plant acclimation: lifetime stomatal frequency response of an individual tree to annual atmospheric CO_2 increase. Proceedings of the National Academy of Sciences of the United States of America 93, 11705–11708.

Wagner, F., Bohncke, S.J.P., Dilcher, D.L., Kürschner, W.M., van Geel, B., Visscher, H., 1999. Century-scale shifts in early Holocene atmospheric CO_2 concentration. Science 284, 1971–1973.

Walker, J.C.G., Hays, P.B., Kasting, J.F., 1981. A negative feedback mechanism for the long-term stabilization of Earth's surface temperature. Journal of Geophysical Research 86, 9776–9782.

Wallman, K., 2001. Controls on the Cretaceous and Cenozoic evolution of seawater composition, atmospheric CO_2 and climate. Geochimica et Cosmochimica Acta (in review).

White, J.W.C., Ciais, P., Figge, R.A., Kenny, R., Markgraf, V., 1994. A high-resolution record of atmospheric CO_2 content from carbon isotopes in peat. Nature 367, 153–156.

Williams-Linera, G., 1997. Phenology of deciduous and broadleaved evergreen tree species in a Mexican tropical lower montane forest. Global Ecology and Biogeography Letters 6, 115–127.

Woodward, F.I., 1986. Ecophysiological studies on the shrub *Vaccinium myrtillus* L. taken from a wide altitudinal range. Oecologia 70, 580–586.

Woodward, F.I., 1987. Stomatal numbers are sensitive to increases in CO_2 from pre-industrial levels. Nature 327, 617–618.

Woodward, F.I., Bazzaz, F.A., 1988. The responses of stomatal density to CO_2 partial pressure. Journal of Experimental Botany 39, 1771–1781.

Woodward, F.I., Kelly, C.K., 1995. The influence of CO_2 concentration on stomatal density. New Phytologist 131, 311–327.

Wright, V.P., Vanstone, S.D., 1991. Assessing the carbon dioxide

content of ancient atmospheres using palaeocalretes: theoretical and empirical constraints. Journal of the Geological Society (London) 148, 945–947.

Wright, V.P., Vanstone, S.D., 1992. Further comments on using carbon isotopes in palaeosols to estimate the CO_2 content of the paleo-atmosphere. Journal of the Geological Society (London) 149, 675–676.

Yapp, C.J., Poths, H., 1992. Ancient atmospheric CO_2 pressures inferred from natural goethites. Nature 355, 342–344.

Yapp, C.J., Poths, H., 1996. Carbon isotopes in continental weathering environments and variations in ancient atmospheric CO_2 pressure. Earth and Planetary Science Letters 137, 71–82.